Spectroscopic Characterization of the Tungsten and Iron Centers in Aldehyde Ferredoxin Oxidoreductases from Two Hyperthermophilic Archaea

Brian P. Koehler,[†] Swarnalatha Mukund,[‡,§] Richard C. Conover,[†,||] Ish K. Dhawan,[†] Roopali Roy,[‡] Michael W. W. Adams,[‡] and Michael K. Johnson*[,†]

Contribution from the Departments of Chemistry and Biochemistry and the Center for Metalloenzyme Studies, University of Georgia, Athens, Georgia 30602

Received June 28, 1996[⊗]

Abstract: The electronic and redox properties of the iron and tungsten centers in the aldehyde ferredoxin oxidoreductases (AORs) from *Pyrococcus furiosus* (Pf) and *Pyrococcus* strain ES-4 (ES-4) have been investigated by the combination of EPR and variable-temperature magnetic circular dichroism (VTMCD) spectroscopies. Parallel- and perpendicular-mode EPR studies of ES-4 AOR reveal a redox inactive "$g = 16$" resonance from an integer spin paramagnet. On the basis of the X-ray crystal structure of Pf AOR (Chan, M. K.; Mukund, S.; Kletzin, A.; Adams, M. W. W.; Rees, D. C. *Science* **1995**, *267*, 1463−1469), this resonance is attributed to a mononuclear high-spin Fe(II) ion at the subunit interface, although the possibility that this center is a carboxylate-bridged reduced diiron center in ES-4 AOR is also considered. Both enzymes have a $[4Fe-4S]^{2+,+}$ cluster with unique electronic properties compared to known synthetic or biological $[4Fe-4S]^{+}$ clusters, i.e. pure $S = {}^3/_2$ ground state with $g = 4.7, 3.4, 1.9$ ($E/D = 0.12$ and $D = +4$ cm^{-1}). Seven distinct W(V) EPR signals have been observed during dye-mediated redox titrations of Pf AOR, and the four major W(V) species have been rigorously identified and characterized via EPR spectral simulations of natural abundance and ^{183}W-enriched samples (^{183}W, $I = {}^1/_2$, 14.28% natural abundance). Both enzymes contain two major forms of W, each corresponding to approximately 20−30% of the total W. One of these is a catalytically competent W species that cycles between the W(IV)/W(V)/W(VI) states at physiologically relevant potentials (<−300 mV) and gives rise to the "low-potential" W(V) resonance, $g \sim 1.99, 1.90, 1.86$. This form of W is quantitatively and irreversibly converted into a distinct and inactive W(IV)/W(V) species by the addition of high concentrations of glycerol or ethylene glycol at 80 °C and is responsible for the "diol-inhibited" W(V) resonance, $g \sim 1.96, 1.94, 1.89$. The other major form of W gives rise to a "high-potential" W(V) species, $g \sim 1.99, 1.96, 1.89$, at nonphysiologically relevant potentials (>0 mV), as a result of a one-electron redox process that is tentatively attributed to ligand based oxidation of a W(VI) species. In addition, active samples of Pf AOR, in particular, can have up to 20% of the W as an inactive W(VI)/W(V) species, with a midpoint potential close to −450 mV, and is responsible for the "spin-coupled" W(V) resonance. This W(V) signal exhibits a broad complex resonance spanning 600 mT due to weak spin−spin interaction with the nearby $S = {}^3/_2$ $[4Fe-4S]^{+}$ cluster. Structures are proposed for each of the major W(V) species on the basis of EPR g values and ^{183}W A values as compared to other biological and synthetic W(V)/Mo(V) centers, VTMCD spectra, and the available X-ray crystallographic and XAS data for Pf AOR and the Mo-containing DMSO reductase from *Rhodobacter sphaeroides*. Comparison with the limited spectroscopic data that are available for all known tungstoenzymes suggests two major classes of enzyme with distinct active site structures.

Introduction

Molybdenum-containing oxotransferases or hydroxylases catalyze a diverse array of redox reactions of the general type

$$X + H_2O \rightleftharpoons XO + 2H^+ + 2e^-$$

with reduction potentials spanning more than 800 mV.[1] The substrate atom on X which is reduced or oxidized can be C (e.g., xanthine oxidase, xanthine dehydrogenase, aldehyde oxidoreductase, CO dehydrogenase, formylmethanofuran dehydrogenase, formate dehydrogenase), N (e.g., nitrate reductase and *N*-oxide reductase), S (e.g., sulfite oxidase, DMSO reductase, and *S*-oxide reductase), or As (e.g., arsenite oxidase). An analogous metabolic role for tungsten has been slow to emerge despite the close similarity in the ionic radii, coordination chemistry, and redox properties of Mo and W. Indeed attempts to replace Mo by W in mesophilic organisms by growth on tungstate led to either inactive molybdoenzymes devoid of Mo or W or inactive W-substituted molybdoenzymes.[2,3] However, studies over the past decade have revealed at least six distinct types of W-containing oxotransferase, all of which are believed to have active sites comprising W coordinated by one or two

[†] Department of Chemistry and Center for Metalloenzyme Studies.
[‡] Department of Biochemistry and Center for Metalloenzyme Studies.
[§] Current address: Recombinant BioCatalysis, Inc., 512 Elmwood Ave., Sharon Hill, PA 19079.
[||] Current address: Department of Cell Biology, Medical College of Georgia, Augusta, GA 30912.
* Address correspondence to this author at the Department of Chemistry, University of Georgia, Athens, GA 30602. Telephone: 706-542-9378. FAX: 706-542-2353. E-mail: johnson@sunchem.chem.uga.edu.
[⊗] Abstract published in *Advance ACS Abstracts,* December 1, 1996.

(1) For recent reviews, see: (a) *Molybdenum Enzymes, Cofactors, and Model Systems*; Stiefel, E. I., Coucouvanis, D., Newton, W. E., Eds.; ACS Symposium Series, Vol. 535; American Chemical Society: Washington, DC, 1993. (b) Young, C. G.; Wedd, A. G. In *Encyclopedia of Inorganic Chemistry*; King, R. B., Ed.; Wiley: U.K., 1994; Vol. 5, pp 2330−2346. (c) Enemark, J. H.; Young, C. G. *Adv. Inorg. Chem.* **1993**, *40*, 1−88. (d) Hille, R. *Biochim. Biophys. Acta* **1994**, *1184*, 143−169.
(2) Johnson, J. L.; Rajagopalan, K. V. *J. Biol. Chem.* **1976**, *251*, 5505−5511.
(3) May, H. D.; Patel, P. S.; Ferry, J. G. *J. Bacteriol.* **1988**, *170*, 3384−3389.

S0002-7863(96)02197-X CCC: $12.00

pterin cofactors[4] in addition to one or more Fe−S cluster.[5] These include aldehyde ferredoxin oxidoreductase (AOR), formaldehyde ferredoxin oxidoreductase (FOR), and glyceraldehyde-ferredoxin oxidoreductase (GAPOR) from hyperthermophilic archeae, formate dehydrogenase (FDH) and carboxylic acid reductase (CAR) from acetogenic bacteria, and formylmethanofuran dehydrogenase (FMDH) from methanogenic archaea. These W-oxotransferases are generally found in thermophilic anaerobes, and all catalyze low-potential conversions (reduction potentials in the range −420 to −560 mV versus NHE) at the level of carboxylic acids and aldehydes.

The recent X-ray crystal structure of the W-containing AOR from the hyperthermophilic archeaon *Pyrococcus furiosus*[6] (Pf) was an important landmark in the continuing efforts to elucidate the active site structure and molecular mechanisms of Mo/W-containing oxotransferases. Not only did this X-ray structure confirm the Rajagopalan model in which the dithiolene side chain of the pterin cofactor coordinates Mo/W,[7] it revealed that two pterin cofactors are coordinated to W and that the dithiolene "side chain" is part of a pyran ring. The tricyclic structure and mode of coordination of the pterin cofactor have since been confirmed by crystallographic results for two molybdenum-containing enzymes, *Desulfovibrio gigas* (Dg) AOR[8] and *Rhodobacter sphaeroides* (Rs) DMSO reductase (DR).[9] However, all three enzymes differ in terms of either the number of coordinated pterin cofactors and/or the presence of a dinucleotide attached by elaboration at the phosphate group. The molybdenum center in Dg AOR is coordinated by a single pterin cofactor with a cytosine dinucleotide, whereas in Rs DR, the molybdenum is coordinated by two pterin cofactors with guanine dinucleotides. In Pf AOR, no protein ligands coordinate the W atom, and the coordination geometry was found to be approximately trigonal prismatic with *cis* glycerol or oxo (or both) ligands completing the W coordination sphere. In addition the X-ray crystal structure confirmed the presence of a [4Fe−4S] cluster and showed it to be in close proximity to the W atom (approximately 10 Å) and connected via H-bond interactions. An unexpected feature of the Pf AOR structure was the presence of a monomeric metal site, tentatively identified as Fe on the basis of anomalous scattering, that bridges the 66-kDa subunits and is coordinated in an approximately tetrahedral arrangement by His and Glu residues arranged in H−X−X−E motifs, one in each subunit.

In contrast to the majority of metalloenzymes, Pf AOR is one of the few instances where crystallography has preceded extensive spectroscopic analysis of the metal centers. Thus far, spectroscopic investigations have largely been confined to UV−visible absorption, EPR investigations,[10] and X-ray absorption (XAS) studies[11] of an inactive form known as the red tungsten protein (RTP) that was isolated before identification of the catalytic function. The EPR data indicated the presence of a center that becomes paramagnetic with an axial $S = {}^3/_2$ ground state on reduction ($E_m = -410$ mV *vs* NHE, at 20 °C and pH 8.0). This center undergoes weak spin−spin interaction with a lower potential center ($E_m = -500$ mV *vs* NHE, at 20 °C and pH 8.0) that also becomes paramagnetic on reduction, to yield a complex spin-spin interaction spectrum spanning 600 mT. Similar EPR properties were observed for active enzyme that was obtained by a rapid purification procedure under more rigorously anaerobic conditions using buffers containing dithiothreitol and glycerol.[12] However, redox titrations were not carried out using active samples and no EPR signals attributable to magnetically isolated W(V) species were observed at this time. Analysis of the W-XAS data for dithionite-reduced RTP indicated a predominant W(VI) oxidation state with two W═O at 1.74 Å, approximately three W−S ligands at 2.41 Å and possibly an additional W−O or W−N ligand at 2.1 Å.[11] The discrepancy between the W-coordination environments deduced from XAS and X-ray crystallography probably results from use of inactive and active samples, respectively, for these measurements. Indeed subsequent W-XAS studies of dithionite-reduced active samples of Pf AOR, analogous to those used for crystallization, indicate a coordination sphere involving one W═O at 1.75 Å, four or five W−S at 2.40 Å, and possibly an additional W−O or W−N at 1.97 Å,[13] which is in good agreement with the crystallographically defined structure.

Now that there is a structural foundation for interpreting the data, there is clearly a pressing need for detailed spectroscopic studies on active samples of Pf AOR using techniques that can selectively probe the W and Fe−S centers. Such studies can then provide a framework for interpreting spectroscopic studies of similar centers in structurally undefined enzymes and for elucidating the electronic and structural changes that occur during the catalytic cycle and upon inactivation. To this end we report here, EPR and variable-temperature magnetic circular dichroism (VTMCD) studies of active and inactive forms of Pf AOR and of a closely related AOR from another strain of *Pyrococcus*, currently termed ES-4.[14] The molecular (size and metal content) and catalytic properties of these two enzymes are indistinguishable within experimental error and their close relationship was confirmed by the high similarity in N-terminal sequences.[14] VTMCD is well established as a means of investigating the ground and excited state properties of paramagnetic Fe−S clusters.[15] More recently it has been shown to provide a selective and sensitive probe for the electronic properties of biological Mo(V) centers,[16] and in this work, we

(4) The term pterin cofactor rather than molybdopterin is used throughout for the modified pterin that coordinates Mo or W in oxotransferases via the dithiolene group in the third ring. This avoids the need to refer to the "tungsten−molybdopterin" active site which is confusing and misleading.

(5) For recent reviews, see: (a) Adams, M. W. W. In *Encyclopedia of Inorganic Chemistry*; King, R. B., Ed.; Wiley: U.K., 1994; Vol. 4, pp 4284−4291. (b) Adams, M. W. W.; Kletzin, A. *FEMS Microbiol. Rev.* **1996**, *18*, 5−63. (c) Johnson, M. K.; Rees, D. C.; Adams, M. W. W. *Chem. Rev.* **1996**, in press.

(6) Chan, M. K.; Mukund, S.; Kletzin, A.; Adams, M. W. W.; Rees, D. C. *Science* **1995**, *267*, 1463−1469.

(7) (a) Rajagopalan, K. V. *Adv. Enzymol. Relat. Areas Mol. Biol.* **1991**, *64*, 215−290. (b) Rajagopalan, K. V.; Johnson, J. L. *J. Biol. Chem.* **1992**, *267*, 10199−10202.

(8) Romão, M. J.; Archer, M.; Moura, I.; Moura, J. J. G.; LeGall, J.; Engh, R.; Schneider, M.; Hof, P.; Huber, R. *Science* **1995**, *270*, 1170−1176.

(9) Schindelin, H.; Kisker, C.; Hilton, J.; Rajagopalan, K. V.; Rees, D. C. *Science* **1996**, *272*, 1615−1621.

(10) Mukund, S.; Adams, M. W. W. *J. Biol. Chem.* **1990**, *265*, 11508−11516.

(11) George, G. N.; Prince, R. C.; Mukund, S.; Adams, M. W. W. *J. Am. Chem. Soc.* **1992**, *114*, 3521−3523.

(12) Mukund, S.; Adams, M. W. W. *J. Biol. Chem.* **1991**, *266*, 14208−14216.

(13) George, G. N.; Mukund, S.; Roy, R.; Adams, M. W. W. Manuscript in preparation.

(14) (a) Johnson, J. L.; Rajagopalan, K. V.; Mukund, S.; Adams, M. W. W. *J. Biol. Chem.* **1993**, *268*, 4848−4852. (b) Mukund, S. Ph.D. Dissertation, University of Georgia, 1995.

(15) (a) Johnson, M. K.; Robinson, A. E.; Thomson, A. J. In *Iron-Sulfur Proteins*; Spiro, T. G., Ed.; Wiley: New York, 1982; pp 367−407. (b) Fu, W.; Drozdzewski, P. M.; Davies, M. D.; Sligar, S. G.; Johnson, M. K. *J. Biol. Chem.* **1992**, *267*, 15502−15510. (c) Conover, R. C.; Kowal, A. T.; Fu, W.; Park, J.-B.; Aono, S.; Adams, M. W. W.; Johnson, M. K. *J. Biol. Chem.* **1990**, *265*, 8533−8541. (d) Onate, Y. A.; Finnegan, M. G.; Hales, B. J.; Johnson, M. K. *Biochim. Biophys. Acta* **1993**, *1164*, 113−123. (e) Finnegan, M. G.; Conover, R. C.; Park, J.-B.; Zhou, Z. H.; Adams, M. W. W.; Johnson, M. K. *Inorg. Chem.* **1995**, 5358−5369.

(16) (a) Finnegan, M. G.; Hilton, J.; Rajagopalan, K. V.; Johnson, M. K. *Inorg. Chem.* **1993**, *32*, 2616−2617. (b) Benson, N.; Farrar, J. A.; McEwan, A. G.; Thomson, A. J. *FEBS Lett.* **1992**, *307*, 169−172. (c) Peterson, J.; Godfrey, C.; Thomson, A. J.; George, G. N.; Bray, R. C. *Biochem. J.* **1986**, *233*, 107−110.

extend this to include W(V) species in AORs. Numerous W(V) species have been observed via their EPR and/or VTMCD spectra and EPR signals have been rigorously identified via ^{183}W-hyperfine splittings ($I = {}^1/_2$, 14% natural abundance) in native and ^{183}W-enriched samples. The ground state g values and hyperfine parameters, as determined by EPR, and the excited state properties, as determined by VTMCD, are compared to those of biological Mo(V)/W(V) centers and Mo(V)/W(V) model complexes containing S-donor ligands. The results reveal considerable heterogeneity at the W center in active preparations of both AORs and suggest that W(VI), W(V), and W(IV) species are all present in dithionite-reduced samples. The W-coordination environment and electronic properties of both active and inactive forms of AOR are discussed in light of the available structural data and electronic properties.

Experimental Section

Sample Preparation. Samples of inactive RTP[10] and active AOR[12] from Pf and active AOR from ES-4[14b] were purified and assayed as previously described. All samples were purified anaerobically in 50 mM Tris/HCl buffer, pH 8.0, with 2 mM sodium dithionite. Active samples of AOR were purified by a rapid purification procedure, and the resulting samples were in the same medium with 2 mM dithiothreitol and 10% (v/v) glycerol.[12] Samples with similar catalytic activities were also purified by the same procedure in the absence of 10% (v/v) glycerol. The active samples used for spectroscopic studies exhibited specific activities in the range 40−60 units/mg, where 1 unit corresponds to 1 μM of crotonaldehyde oxidized/min at 80 °C. Inactive Pf RTP samples exhibited specific activities of <1 unit/mg. The sample concentrations quoted in the figure legends are based on protein determinations using the Lowry method, with a correction factor applied based on direct amino acid analysis, and are expressed per monomer ($M_r = 67\,000$). ^{183}W-enriched samples of Pf AOR were purified from cells grown on a medium containing 10 μM $Na_2{}^{183}WO_4$ (90% ^{183}W enrichment, Cambridge Isotope Laboratories). Samples were handled in a Vacuum Atmospheres glovebox (<1 ppm O_2) under an argon atmosphere.

EPR redox titrations were performed at ambient temperature (25−27 °C) in the glovebox under anaerobic conditions using a 100 mM Tris-HCl buffer, pH 7.8. Mediator dyes were added, each to a concentration of ca. 50 μM, in order to cover the desired range of redox potentials, i.e. methyl viologen, benzyl viologen, neutral red, safranin O, phenosafranin, anthraquinone-2-sulfonate, anthraquinone-1,5-disulfonate, 1,4-benzoquinone, indigodisulfonate, 1,2-naphthoquinone, thionine, methylene blue, duroquinone, and 1,2-naphthoquinone-4-sulfonate. Samples were first reduced by addition of excess sodium dithionite followed by oxidative titration with potassium ferricyanide. After equilibration at the desired potential, a 0.2-mL aliquot was transferred to a calibrated EPR tube and immediately frozen in liquid nitrogen. Potentials were measured with a platinum working electrode and a saturated Ag/AgCl reference electrode. All redox potentials are reported relative to NHE.

Spectroscopic Methods. Absorption spectra were recorded on either a Shimadzu UV301PC or Varian DMS 200 spectrophotometer. Variable-temperature and variable-field MCD measurements were recorded on samples containing 50−70% (v/v) ethylene glycol or glycerol using a Jasco J-500C (180−1000 nm) or J-730 (700−2000 nm) spectropolarimeter mated to an Oxford Instruments SM3 (0−5 T) or Spectromag 4000 (0−7 T) split-coil superconducting magnet. The experimental protocols for measuring MCD spectra of oxygen-sensitive samples over the temperature range 1.5−300 K with magnetic fields up to 7 T have been described elsewhere.[17] X-band (~9.6 GHz) EPR spectra were recorded on a Bruker ESP-300E EPR spectrometer with a dual mode ER-4116 cavity and equipped with an Oxford Instruments ESR-9 flow cryostat (4.2−300 K). Frequencies were measured with a Systron-Donner 6054B frequency counter, and the field was calibrated with a Bruker ER 035M gaussmeter. Spin quantitations were carried out under nonsaturating conditions using 1 mM CuEDTA as the standard. Simulations of frozen solution EPR spectra were carried out using a modified version of the QPOW program developed by Prof. R. L. Belford and co-workers.[18] The $I = {}^1/_2$ (^{183}W isotope, 14.28% natural abundance) and $I = 0$ (^{182,184,186}W isotopes, 85.72% natural abundance) components were simulated separately and then summed in the appropriate ratio to obtain simulations of the natural abundance spectra.

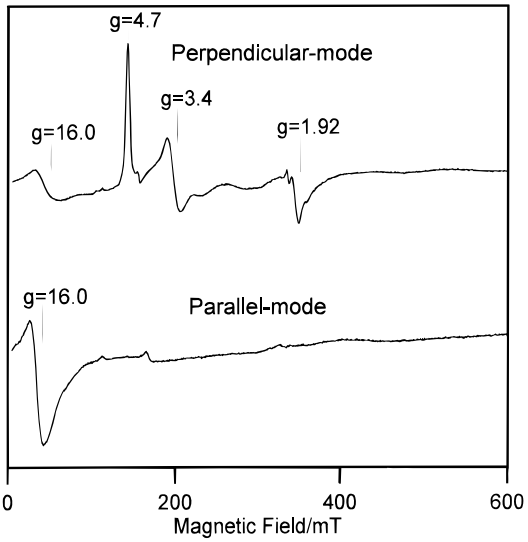

Figure 1. Perpendicular-mode and parallel-mode X-band EPR spectra of dithionite-reduced ES-4 AOR. The sample was 0.15 mM in AOR. EPR conditions: temperature, 4.2 K; microwave power, 10 mW; modulation amplitude, 0.63 mT; microwave frequency, 9.60 GHz (perpendicular mode) and 9.37 GHz (parallel-mode).

Results

Dithionite-Reduced *P. furiosus* and ES-4 AORs. Samples of inactive RTP and active AOR from Pf and active AOR from ES-4 were investigated as-prepared in the presence of 2 mM dithionite. They exhibited EPR and VTMCD spectra with common features, but with some interesting and revealing differences. EPR spectra of ES-4 AOR obtained in both parallel-mode (microwave magnetic field parallel to the applied field) and the more conventional perpendicular-mode (microwave magnetic field perpendicular to the applied field) are shown in Figure 1. The perpendicular-mode spectrum is dominated by a rhombic resonance, $g = 4.7$, 3.4, 1.9, that is characteristic of a $S = {}^3/_2$ ground state. This resonance is readily interpreted in terms of a conventional isotropic $S = {}^3/_2$ spin Hamiltonian

$$H_e = g_0\beta\mathbf{H}\cdot\mathbf{S} + D(S_z^2 - S(S+1)/3) + E(S_x^2 - S_y^2)$$

which predicts effective g values of 4.66, 3.25, and 1.92 for the "$M_s = \pm{}^1/_2$" doublet and 5.92, 0.75, and 0.66 for the "$M_s = \pm{}^3/_2$" doublet with $g_0 = 2.0$ and $E/D = 0.12$. A weak, sharp resonance at $g = 6.0$ is observable between 8 and 15 K and temperature-dependence studies over this range indicate that it arises from the upper doublet. Plots of the log of the ratio of the intensities at $g = 6.0$ and 4.7 as a function of $1/T$ (not shown) are linear within experimental error and the slope is consistent with $D = +4.0 \pm 0.5$ cm^{-1}. Weak additional features at $g \sim$ 10, 2.8, 2.3, and 1.3 were observable at high microwave powers and low temperatures (≥10 mW and 4.2 K) in some, but not

(17) (a) Johnson, M. K. In *Metal Clusters in Proteins*; Que, L., Jr., Ed.; ACS Symposium Series, Vol. 372; American Chemical Society: Washington, DC, 1988; pp 326−342. (b) Thomson, A. J.; Cheeseman, M. R.; George, S. J. *Methods Enzymol.* **1993**, *226*, 199−232.

(18) (a) Belford, R. L.; Nilges, M. J. Computer Simulation of Powder Spectra. EPR Symposium, 21st Rocky Mountain Conference, Denver, CO, 1979. (b) Nilges, M. J. Ph.D. Dissertation, University of Illinois, Urbana, IL, 1979.

all, preparations of active ES-4 AOR. These features are similar to those that dominate the spectrum of inactive Pf RTP, see below. All samples of ES-4 AOR exhibited a derivative-shaped feature centered around $g \sim 16$, that sharpened and increased in intensity in parallel mode and increased in intensity with decreasing temperature down to at least 4.2 K. Such properties are uniquely indicative of an integer spin paramagnet, i.e. $S \geq 1$, with resonance occurring between the lowest energy components of the ground state manifold.[19] On the basis of the X-ray structure of Pf AOR,[6] this signal is tentatively assigned to a resonance within the "$M_s = \pm 2$ doublet" of a high-spin Fe(II) site ($S = 2$ and $D < 0$) located at the subunit interface. In accord with their assignment to half-integer spin systems, all other resonances are lost in parallel mode.

VTMCD spectra of a sample of ES-4 AOR containing 55% (v/v) glycerol and exhibiting only the $g = 16$ and $S = {}^3/_2$ resonances are shown in Figure 2a. VTMCD spectra provide a useful "fingerprint" of cluster type for paramagnetic Fe−S centers,[15] and the pattern of bands for dithionite-reduced ES-4 AOR are characteristic of a $S = {}^3/_2$ [4Fe−4S]$^+$ cluster similar to those found in Pf ferredoxin (Fd)[15c] and urea-treated nitrogenase Fe protein.[15d] That the MCD intensity originates from transitions arising from the EPR-detectable $S = {}^3/_2$ ground state is demonstrated by MCD saturation magnetization studies (see Supporting Information). At 1.62 K, when only the lowest doublet of zero-field-split manifold is significantly populated, MCD saturation magnetization plots are well fit by theoretical data constructed for an *xy*-polarized transition from a doublet with $g_\perp = 4.0$ and $g_\parallel = 2.0$,[20] i.e. the $M_s = \pm {}^1/_2$ doublet of a $S = {}^3/_2$ ground state with axial zero-field splitting ($D > 0$).

EPR spectra of as-prepared samples of inactive RTP and active AOR from Pf recorded at 4.2 K are compared in Figure 3. In contrast to ES-4 AOR, all resonances were lost and no additional resonances appeared in parallel-mode studies of Pf RTP and AOR. The spectrum shown for reduced RTP, Figure 3a, is in excellent agreement with the previously published data, which were interpreted in terms of two overlapping resonances based on extensive redox titrations as a function of pH.[10] One resonance originates from an $S = {}^3/_2$ species, $g = 4.7$, 3.4, 1.9, with identical properties to those deduced above for dithionite-reduced ES-4 AOR. The other is a broad, complex resonance spanning almost 600 mT with inflections at $g = 10.0$, 6.5, 5.4, 3.6, 2.9, 2.3, 1.8, 1.6, and 1.3. This complex resonance was attributed to weak spin−spin interaction between the $S = {}^3/_2$ center and a lower potential center that becomes paramagnetic only on one-electron reduction.[10] All active AOR samples investigated in this work exhibited a similar complex resonance, but the intensity of this resonance relative to the $S = {}^3/_2$ resonance was invariably much less than in inactive RTP for equivalent sample and EPR conditions. Care must be taken in comparing the intensity of these resonances since the relative intensity of the $S = {}^3/_2$, and the broad complex resonance in RTP is critically dependent on the pH and poised potential of the solution.[10] However, redox titrations of active AOR, see below, confirmed that the intensity of the broad complex resonance is intrinsically reduced by a factor of 5−10-fold in active AOR compared to inactive RTP samples.

The origin of the $S = {}^3/_2$ center and the nature and spin state of the lower potential species were left unresolved in the earlier work.[10] The MCD studies of the analogous $S = {}^3/_2$ center in ES-4 AOR reported above, coupled with the X-ray structure of Pf AOR,[6] clearly identify the $S = {}^3/_2$ center as a [4Fe−4S]$^+$ cluster with complete cysteinyl coordination. Since the W center is in close proximity to the [4Fe−4S] cluster (the closest distance between metals is ~8 Å),[6] spin−spin interaction between the $S = {}^3/_2$ [4Fe−4S]$^+$ cluster and a $S = {}^1/_2$ W(V) species is an attractive interpretation for the complex resonance. The only alternative possibility is spin coupling between the $S = {}^3/_2$ [4Fe−4S]$^+$ cluster and a nearby protein-based or pterin-based $S = {}^1/_2$ radical species. However, EPR studies of ^{183}W-enriched samples of active AOR and VTMCD studies of inactive RTP argue strongly in favor of a W(V) species.

First the dominant well-resolved features centered at $g = 2.9$ and 2.3 show significant broadening (6−8 mT) in ^{183}W-enriched samples, cf. Figure 3b,c, indicating that the electronic spin is coupled to a W nucleus. Second, the VTMCD spectrum of dithionite-reduced RTP, Figure 2b, shows additional bands compared to the spectrum obtained for the equivalent $S = {}^3/_2$ [4Fe−4S]$^+$ cluster in ES-4 AOR, Figure 2a. A direct comparison is shown in Figure 4, along with a difference spectrum that approximates the temperature dependent MCD spectrum of the paramagnetic species responsible for the complex spin−spin interaction EPR signal. MCD saturation magnetization studies of Pf RTP were carried out at 550, 520, and 470 nm. The data at 520 nm are readily interpreted in terms of a 20:80 mixture of transitions arising from $S = {}^1/_2$ and $S = {}^3/_2$ ground states, respectively (see Supporting Information). The data at 550 and 470 nm were both analyzed in the same way in terms of a 60:40 mixture of transitions originating from $S = {}^1/_2$ and $S = {}^3/_2$ ground states, respectively. Hence the MCD saturation magnetization data indicates a $S = {}^1/_2$ ground state for the paramagnetic species interacting with the $S = {}^3/_2$ [4Fe−4S]$^+$ cluster. Due to small spin-orbit coupling, $S = {}^1/_2$ radical species invariably give rise to very weak temperature-dependent MCD compared to paramagnetic transition metal centers and the intensity of the difference spectrum is clearly inconsistent with such an assignment. In contrast, a $S = {}^1/_2$ W(V)-dithiolene center would be expected to exhibit intense temperature-dependent S → W(V) charge transfer MCD bands in the visible region due to the large spin−orbit coupling associated with third row transition elements. Hence the difference MCD spectrum shown in Figure 4 is attributed to a W(V) species with a W(V)/W(VI) midpoint potential less than the [4Fe−4S]$^{2+/+}$ couple. However, since the complex EPR signal is present to a much lesser extent in active samples of AORs, it almost certainly corresponds to a catalytically inactive W species.

Active samples of Pf AOR also exhibited distinctive VTMCD spectra compared to inactive RTP, cf. Figure 2b,c. The major differences are additional positive bands centered at 485 and 380 nm and magnetization data at these wavelengths clearly demonstrated that the additional paramagnetic chromophore has a $S = {}^1/_2$ ground state. This prompted a thorough EPR investigation of the samples used for VTMCD studies which contained 55% (v/v) glycerol. At 4.2 K, the EPR spectrum was the same as that exhibited by samples containing 10% (v/v) glycerol, see Figure 3b, but a slow-relaxing, rhombic, $S = {}^1/_2$ resonance, $g = 1.965$, 1.941, 1.884, accounting for 0.02 spins/W was observed at temperatures of >30 K. The EPR resonance and the associated VTMCD bands were enhanced at least 5-fold in dithionite-reduced samples poised at a higher potential by using a 50 mM MES buffer, pH 6.3, with 55% (v/v) glycerol. (The resulting VTMCD spectra were almost identical in form, but with $\Delta\epsilon$ values approximately half of those shown in Figure 2d). These unique EPR and VTMCD attributes were not observed in samples of inactive RTP at pH 7.8 or 6.3, indicating

(19) (a) Hagen, W. R. *Biochim. Biophys. Acta* **1982**, *708*, 82−98. (b) Hendrich, M. P.; Debrunner, P. G. *J. Magn. Reson.* **1988**, *78*, 133−141. (c) Hendrich, M. P.; Debrunner, P. G. *Biophys. J.* **1989**, *56*, 489−506.

(20) (a) Thomson, A. J.; Johnson, M. K. *Biochem. J.* **1980**, *191*, 411−420. (b) Bennett, D. E.; Johnson, M. K. *Biochim. Biophys. Acta* **1987**, *911*, 71−80.

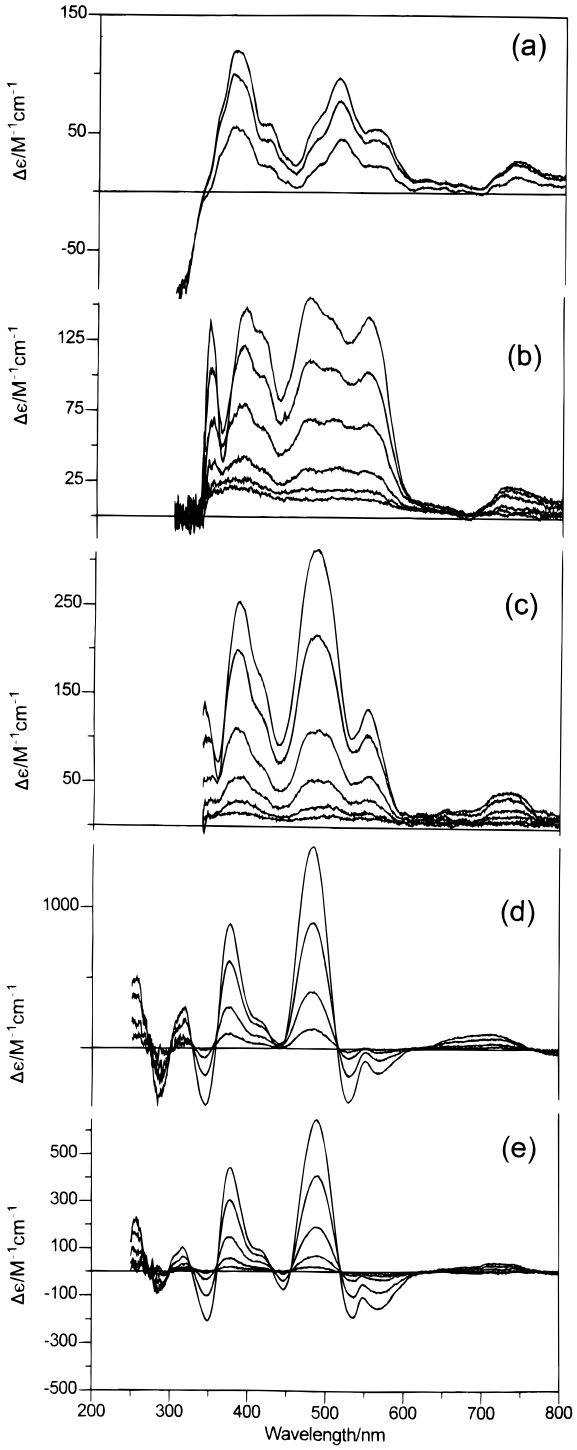

Figure 2. VTMCD spectra of samples of dithionite-reduced ES-4 and Pf AOR. (a) Active ES-4 AOR, 0.11 mM in AOR with 55% (v/v) glycerol. Spectra recorded at temperatures of 1.62, 4.22, and 9.7 K. (b) Pf RTP (inactive AOR), 0.20 mM in AOR with 55% (v/v) glycerol. Spectra recorded at temperatures of 1.61, 4.22, 8.6, 21, 51, and 91 K. (c) Active Pf AOR, 0.14 mM in AOR with 50% (v/v) glycerol. Spectra recorded at temperatures of 1.66, 4.22, 10.2, 20, 55, and 99 K. (d) Active Pf AOR heated to 80 °C and incubated with formaldehyde for 5 min followed by addition of glycerol at 80 °C. The final solution was 0.08 mM in AOR, and contained 2 mM formaldehyde and 70% (v/v) glycerol. Spectra recorded at temperatures of 1.68, 4.22, 9.8, and 18.6 K. (e) As in d except that ethylene glycol was used in place of glycerol. The final solution was 0.10 mM in AOR, and contained 2 mM formaldehyde and 60% (v/v) ethylene glycol. Spectra recorded at temperatures of 1.71, 4.22, 10.2, 22, and 50 K. For each sample, the MCD spectra were recorded with an applied magnetic field of 4.5 T and the intensity of all transitions increases with decreasing temperature.

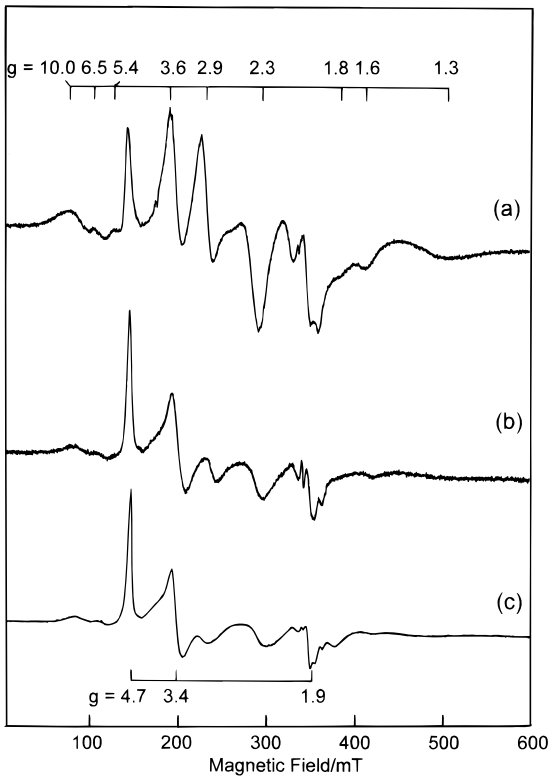

Figure 3. X-band EPR spectra of inactive and active (natural abundance and ^{183}W-enriched) dithionite-reduced Pf AOR: (a) RTP (inactive AOR); (b) Active AOR; (c) Active AOR enriched with ^{183}W (80−90% enrichment). The samples were all 0.2−0.3 mM in AOR. EPR conditions: temperature, 4.2 K; microwave power, 1 mW; modulation amplitude, 0.63 mT; microwave frequency, 9.59 GHz.

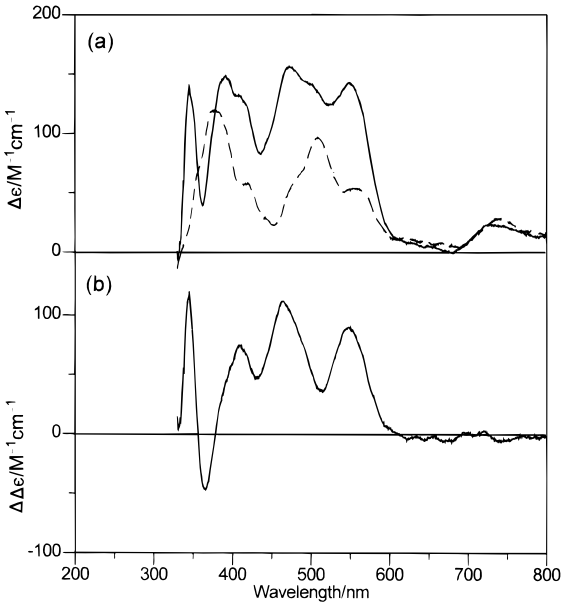

Figure 4. Comparison of the VTMCD spectra of dithionite-reduced Pf RTP and ES-4 AOR. (a) VTMCD spectra of dithionite-reduced Pf RTP (solid line) and dithionite-reduced ES-4 AOR (dashed line) at 4.2 K and 4.5 T. The samples are described in Figure 2a,b. (b) Pf RTP minus ES-4 AOR VTMCD difference spectrum.

that the species responsible is uniquely associated with active AOR. The VTMCD and EPR properties (i.e., intense temperature-dependent visible MCD from a $S = {}^1/_2$ chromophore and slow relaxing $S = {}^1/_2$ resonance with $g_{av} < 2$) are clearly indicative of a magnetically isolated W(V) species and this assignment was subsequently confirmed by EPR studies of ^{183}W-enriched samples, see below. This was the first evidence for

magnetically isolated W(V) species in active AORs and lead to comprehensive VTMCD and EPR studies on the effects of substrate, glycerol/ethylene glycol, and redox potential on the W center in active Pf and ES-4 AORs.

Formaldehyde-Treated *P. furiosus* and ES-4 AORs. Initial attempts to induce magnetically-isolated W(V) species in AORs centered on the addition of substrate, formaldehyde, at temperatures approaching physiological conditions. Samples of dithionite-reduced Pf AOR with glycerol removed from the storage buffer by ultrafiltration, were heated to 80 °C under strictly anaerobic conditions. After incubation with formaldehyde (2 mM), a sample was frozen for EPR studies and 60−70% (v/v) glycerol or ethylene glycol (heated to 80 °C) was added to the remaining sample prior to freezing for EPR and VTMCD studies. The samples treated with glycerol or ethylene glycol exhibited only residual activity (<5%), even after removal of the large excess of diol by ultrafiltration or dilution. All three samples exhibited 4.2 K EPR spectra essentially identical to that shown in Figure 3b for dithionite-reduced active AOR. However, each exhibited distinct rhombic $S = {}^1/_2$ resonances at 50 K: $g = 1.989$, 1.901, and 1.863 (low-potential W(V) species; 0.12 spins/W) for the sample without glycerol or ethylene glycol; $g = 1.965$, 1.941, and 1.884 (glycerol-inhibited W(V) species; 0.22 spins/W) for the sample with 70% (v/v) glycerol; $g = 1.958$, 1.938, and 1.887 (glycol-inhibited W(V) species; 0.17 spins/W) for the sample treated with 60% (v/v) ethylene glycol; see Figure 5. Parallel EPR studies with ^{183}W-enriched samples of Pf AOR revealed resolved ^{183}W-hyperfine on each of the principal g values, showing that all three resonances originate from magnetically isolated W(V) species. Figure 6a,b shows experimental and simulated ^{NA}W- and ^{183}W-enriched EPR spectra for the low-potential and glycerol-inhibited W(V) species, respectively. The ^{183}W-enriched samples facilitated accurate estimates of the ^{183}W-hyperfine coupling constants, see Table 1, and reliable simulations of the natural abundance spectra (14% ^{183}W, $I = {}^1/_2$). These W(V) resonances were not observed in analogous experiments with inactive Pf RTP samples.

The glycerol-inhibited W(V) species exhibited an intense VTMCD spectra, see Figure 2d, with pronounced positive bands centered at 485 and 380 nm. Formaldehyde treatment optimized the amount of the glycerol-inhibited W(V) species but is clearly not required to produce this species, since analogous EPR and VTMCD spectra were observed for dithionite-reduced Pf AOR samples at pH 6.3 in the presence of 55% (v/v) glycerol, see above. Very similar VTMCD spectra were also observed when glycerol was replaced by ethylene glycol, with the only significant differences being 1−6-nm red shifts in the dominant bands and a more pronounced negative band centered at 446 nm for the glycol-inhibited W(V) species, Figure 2e. MCD saturation magnetization studies for the glycerol-treated sample confirmed that the observed bands originate exclusively from a chromophore with a $S = {}^1/_2$ ground state (see Supporting Information). Hence the VTMCD spectrum of the glycerol-inhibited W(V) species overwhelmingly dominates that of the $S = {}^3/_2$ $[4Fe-4S]^+$ cluster at low temperatures. Indeed, on a per-center basis, the $\Delta\epsilon$ values for the diol-inhibited W(V) species are at least 30-fold greater than for the $[4Fe-4S]^+$ cluster or the spin-coupled W(V) species. The small but significant differences in the VTMCD and EPR properties of the glycerol-induced and ethylene-glycol-induced W(V) species clearly point to direct interaction of these diols at the W center to yield closely related species.

Redox Titrations of *P. furiosus* and ES-4 AORs. Magnetically-isolated W(V) species were not observed in EPR-monitored redox titrations of Pf RTP.[10] In contrast, numerous W(V) EPR signals were observed in oxidative redox titrations of active samples of Pf AOR and preliminary studies indicate that equivalent species are also present in ES-4 AOR. The EPR parameters and redox properties of all the W(V) species observed are summarized in Table 1, and EPR spectra for Pf AOR at selected poised potentials are shown in the Supporting Information. Redox titrations with Pf AOR were carried out at pH 7.8 with samples purified in the presence of 10% (v/v) glycerol, after removal of glycerol by anaerobic ultrafiltration, and purified in the absence of glycerol. Figure 7 shows plots of the intensity of individual resonances as a function of potential with fits to one-electron Nernst plots.

The redox behavior of the spin-coupled W(V) species and the $S = {}^3/_2$ $[4Fe-4S]^+$ cluster were monitored at 4.2 K, and analogous results were observed in all three redox titrations, i.e. spin-coupled W(VI)/W(V), $E_m = -443 \pm 20$ mV, and $[4Fe-4S]^{2+/+}$, $E_m = -350 \pm 20$ mV. The complex resonance associated with the spin-coupling between $S = {}^1/_2$ W(V) and $S = {}^3/_2$ $[4Fe-4S]^+$ centers was fully developed at the lowest potentials obtainable, ∼−550 mV, but in contrast to RTP,[10] this

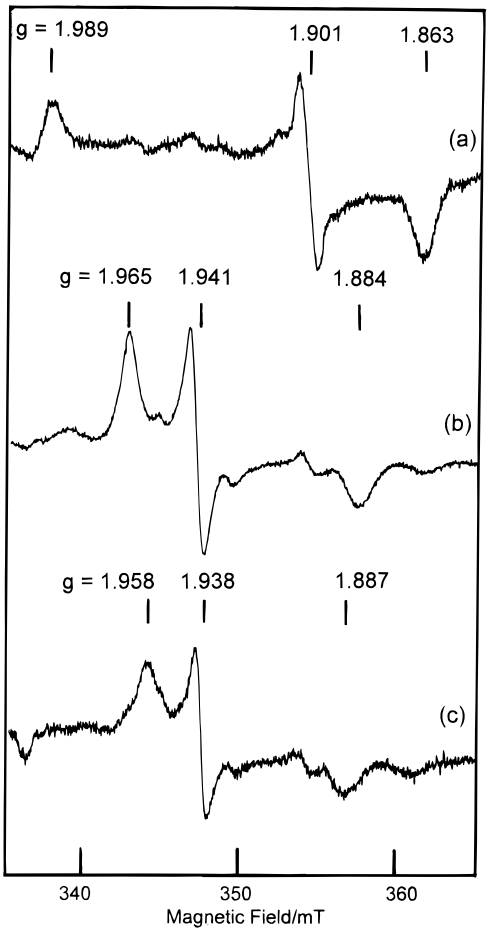

Figure 5. Comparison of W(V) EPR spectra for active dithionite-reduced Pf AOR treated with formaldehyde at 80 °C. Glycerol was removed from the purification buffer by ultrafiltration, and the samples were heated to 80 °C, treated with 2 mM formaldehyde, and incubated for 5 min prior to freezing or treatment with glycerol or ethylene glycol at 80 °C followed by freezing. (a) No glycerol or ethylene glycol. The sample concentration was 0.240 mM, and the spin concentration was 0.12 spins/W. (b) In the presence of 70% (v/v) glycerol. The sample is described in Figure 2d, W(V) spin concentration = 0.22 spins/W. (c) In the presence of 60% (v/v) ethylene glycol. The sample is described in Figure 2e, W(V) spin concentration = 0.17 spins/W. EPR conditions: temperature, 50 K; microwave power, 10 mW; modulation amplitude, 0.63 mT; microwave frequency, 9.44 GHz.

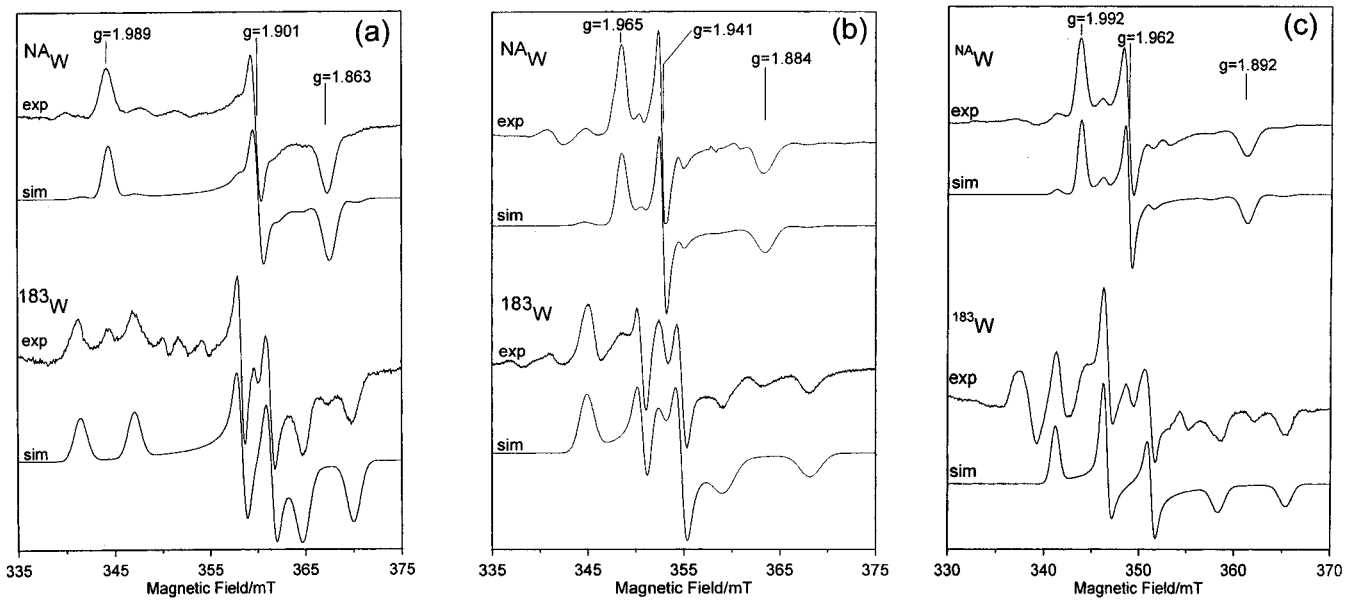

Figure 6. ^{NA}W- and ^{183}W-enriched EPR spectra and simulations of the low-potential (a), glycerol-inhibited (b) and high-potential (c) W(V) species in Pf AOR. The low-potential and glycerol-inhibited samples were prepared as described in Figure 5 parts a and b, respectively. The high-potential samples contained 10% (v/v) glycerol and were poised at +250 mV (*vs* NHE) by ferricyanide oxidation in the presence of redox dyes. Only the ^{183}W component is simulated in the ^{183}W-enriched samples (enrichment estimated at 80−90%), and the resulting parameters were used to simulate the ^{NA}W spectra (14.3% $I = {}^1/_2$ ^{183}W; 85.7% $I = 0$ W isotopes). The simulation parameters were: (a) $g_{1,2,3} = 1.989, 1.901, 1.863$; $A_{1,2,3} = 52, 28, 46 \times 10^{-4}$ cm^{-1}; $l_{1,2,3} = 0.79, 0.51, 0.80$ mT; (b) $g_{1,2,3} = 1.965, 1.941, 1.884$; $A_{1,2,3} = 67, 37, 79 \times 10^{-4}$ cm^{-1}; $l_{1,2,3} = 1.00, 0.51, 1.17$ mT; (c) $g_{1,2,3} = 1.992, 1.962, 1.892$; $A_{1,2,3} = 48, 43, 62 \times 10^{-4}$ cm^{-1}; $l_{1,2,3} = 0.50, 0.41, 0.75$ mT; where l is the line width. EPR conditions: temperature, 40 K; microwave power, 1 mW; modulation amplitude, 1.02 mT; microwave frequency, 9.60 GHz.

Table 1. EPR g Values, ^{183}W A Values (cm^{-1} × 10^4), and Midpoint Potentials (mV *vs* NHE) for W(V) Species in *P. furiosus* and *Pyrococcus* sp. ES-4 AORs

									E_m (pH 7.8)	
sample/species	g_{av}	A_{av}	g_1	g_2	g_3	A_1	A_2	A_3	W^{IV}/W^V	W^V/W^{VI}
P. furiosus AOR										
spin-coupled									<−550	−443
low-potential[a]	1.918	42	1.989	1.901	1.863	52	27	46	−436	−365
glycerol-inhibited[a]	1.930	61	1.965	1.941	1.884	67	37	79	−355	>+100
glycol-inhibited[a]	1.928	60	1.958	1.938	1.887	66	35	79	n.d.[b]	n.d.
mid-potential	1.963		1.988	1.961	1.940				−345	>+100
high-potential[a]	1.949	51	1.992	1.962	1.892	48	43	62	+157	>+300
re-reduced 1	1.989		2.021	1.988	1.957				Optimal at ∼−190 mV	
re-reduced 2	1.905		1.949	1.916	1.850				Optimal at ∼−190 mV	
Pyrococcus sp. ES-4 AOR										
low-potential	n.d.		n.d.	1.900	1.860				−385	−310
glycerol-inhibited	1.927		1.961	1.940	1.881				−315	>+300
high-potential	1.945		1.986	1.960	1.890				+50	>+300

[a] g values (±0.001) and A values (± 2 × 10^{-4} cm^{-1}) determined by simulation of natural abundance and ^{183}W-enriched spectra. [b] n.d., not determined.

resonance is a very minor component at this potential compared to the magnetically-isolated $S = {}^3/_2$ resonance. Consequently there was no significant decrease in the intensity of the $S = {}^3/_2$ resonance associated with the appearance of the complex resonance and the redox data can be fit to a good approximation with simple one-electron Nernst plots. A $g = 4.3$ resonance from a rhombic high-spin Fe(III) species ($E/D \sim 0.33$) appeared with a midpoint potential of +110 ± 20 mV. However, approximate quantitation (using the $g = 4.3$ resonance of an aqueous high-spin Fe(III) standard, but without correction for possible differences in zero-field splitting) indicates this is a minor component corresponding to <10% of the enzyme concentration. Therefore, it is attributed to adventitiously bound Fe(III) ion rather than oxidation of the mononuclear Fe(II) center at the subunit interface, and this assignment is supported by redox titrations on ES-4 AOR, see below.

The redox behavior of magnetically-isolated W(V) species was monitored at 50 K. As the potential is increased, the low-potential W(V) resonance, $g = 1.989, 1.901, 1.863$, analogous to that seen above in formaldehyde-treated samples, see Figures 5a and 6a, increases and subsequently decreases. (The low-field component of the resonance is obscured by radicals from the redox dyes used in the titration.) This resonance reaches a maximum at around −400 mV, and the intensity is glycerol-dependent. It was maximal for samples purified in the absence of glycerol and spin quantitations of appropriately scaled simulated spectra indicate a maximum intensity corresponding to 0.15 ± 0.02 spins/W. The redox behavior was fit to a Nernst expression derived for two sequential one-electron oxidations with only the one-electron oxidized form EPR active, $E_m(W(IV)/W(V)) = -436 \pm 20$ mV and $E_m(W(V)/W(VI)) = -365 \pm 20$ mV. Taken together with the spin quantitation data, this indicates that the W center responsible for the low-potential W(V) species corresponds to between 20 and 30% of the W in the enzyme purified in the absence of glycerol.

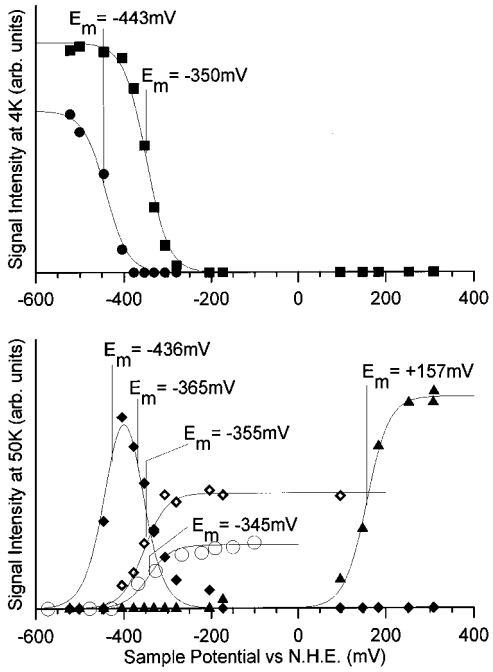

Figure 7. EPR signal intensities (arbitrary units) for Pf AOR as a function of poised potential. Dye-mediated redox titrations were carried out as described in the Experimental Section with active Pf AOR (0.07 mM) purified in the presence of 10% (v/v) glycerol, except where otherwise indicated. Upper panel: intensity of the $g = 4.7$ component of $S = {}^3/_2$ $[4Fe-4S]^+$ cluster (■) and the $g = 2.9$ component of the spin-coupled W(V) species (●) at 4.2 K. Lower panel: peak-to-trough intensity of the $g = 1.901$ feature of the low-potential W(V) species (◆), peak-to-trough intensity of the $g = 1.941$ component of the glycerol-inhibited W(V) species (◇), intensity of the $g = 1.892$ component of the high-potential W(V) species (▲), intensity of the $g = 1.940$ component of the mid-potential W(V) species (sample purified in absence of glycerol, 0.06 mM in AOR) (○), all measured at 50 K. Solid lines are best fits to one-electron Nernst equations or a two-electron Nernst equation for sequential one-electron oxidations with only the one-electron oxidized form EPR active. The midpoint potentials (*vs* NHE) used in constructing the Nernst plots are indicated on the figure. EPR conditions: temperatures as indicated; microwave power, 1 mW; modulation amplitude, 1.02 mT; microwave frequency, 9.60 GHz.

In the presence of increasing amounts of glycerol, the W species responsible for the low-potential W(V) resonance appears to be quantitatively converted into a new species that gives rise to the glycerol-inhibited W(V) species, $g = 1.965$, 1.941, 1.884, see Figures 5b and 6b, on one-electron oxidation, $E_m(W(IV)/W(V)) = -355 \pm 20$ mV. Both the low-potential and the glycerol-inhibited W(V) species were observed in redox titrations of samples isolated in the presence of 10% (v/v) glycerol. In accord with the EPR data for formaldehyde-treated samples discussed above, preliminary redox titrations in the presence of 60% (v/v) glycerol showed negligible amounts of the low-potential W(V) species, but exhibited an intense glycerol-inhibited W(V) signal, accounting for 0.30 ± 0.05 spins/W in samples poised around −200 mV. Moreover, the glycerol-inhibited W(V) species persists even in samples even after glycerol has been removed. For example, redox titrations conducted on samples prepared in the presence of 10% (v/v) glycerol, but subsequently stripped of glycerol by anaerobic ultrafiltration, were identical to those shown obtained prior to removal of glycerol and still showed the glycerol-inhibited EPR signal.

Two additional W(V) EPR resonances were observed in oxidative redox titrations at higher potentials, irrespective of the presence of glycerol. One, termed the mid-potential W(V) species, $g = 1.988$, 1.961, 1.940, appears with a midpoint potential of -345 ± 20 mV and persists up to at least +100 mV (at higher potentials the EPR spectrum in this region is dominated by more intense high-potential W(V) species discussed below). It is most readily seen in samples purified in the absence of glycerol at potentials between −250 and +50 mV but was also observable in addition to the glycerol-induced W(V) species in samples purified with 10% (v/v) glycerol (see Supporting Information). However, in all preparations it is a minor species accounting for <0.03 spins/W. A much more intense W(V) resonance accounting for 0.30 ± 0.05 spins/W and termed the high-potential W(V) species, $g = 1.992$, 1.962, 1.892, appears with a midpoint potential of $+157 \pm 20$ mV and persists up to at least +300 mV. ^{183}W-hyperfine is resolved even in the natural abundance spectrum and parallel studies of ^{183}W-enriched samples afford accurate estimates of the ^{183}W coupling constants and reliable spectral simulations, see Figure 6c and Table 1. The same W(V) resonance was also observed in samples of active Pf AOR that were oxidized and irreversibly inactivated by exposure to O_2 for 1 h at room temperature. Hence, this resonance does not arise from a catalytically competent W(V) species.

The results thus far have involved oxidative redox titrations. To assess reversibility, a more limited set of data points was obtained under reducing conditions for the sample purified in the absence of glycerol. This established that the oxidative redox processes occurring up to 0 mV are all fully reversible and no new signals were observed under reducing conditions for samples that were not oxidized at potentials higher than 0 mV. Furthermore, there was no significant loss in activity for samples that were not exposed to potentials of >0 mV. In contrast, enzymatic activity was completely lost and two new EPR resonances, $g = 2.021$, 1.988, 1.957 (re-reduced 1) and 1.949, 1.916, 1.850 (re-reduced 2), were observed under reducing conditions in samples that had been anaerobically oxidized to +300 mV. The g values and relaxation properties are indicative of W(V) species. These W(V) species appeared transiently during re-reduction, both being maximal at approximately −190 mV, but they were readily resolved on the basis of different temperature-dependent behaviors (see Supporting Information). Taken together these resonances maximally accounted for 0.25 ± 0.05 spins/W. Re-reduction of samples oxidized to +300 mV involved loss of the high-potential and mid-potential W(V) signals at midpoint potentials within experimental error of those established in the oxidative titrations, but the low-potential W(V) resonance was not observed. The results are interpreted in terms of an irreversible redox process, occurring at potentials of >0 mV, and involving the W species responsible for the low-potential W(V) resonance. Moreover, they strongly suggest that this W species is responsible, at least in part, for enzymatic activity.

The properties of the high-potential W(V) species were also investigated by VTMCD spectroscopy. This was accomplished by adding 55% (v/v) glycerol to the sample poised at +309 mV and freezing for parallel EPR and VTMCD studies. The EPR spectrum was unchanged by the addition of glycerol and the resulting sample exhibited the high-potential W(V) resonance accounting for approximately 0.30 ± 0.03 spins/W. The corresponding VTMCD spectrum is shown in Figure 8, together with that of the glycerol-induced W(V) species in order to facilitate direct comparison. MCD magnetization studies confirm a $S = {}^1/_2$ ground state for all transitions and near-IR studies reveal an additional negative band centered at 880 nm. The VTMCD spectrum for the high-potential W(V) species is composed of four sets of alternate negative and positive temperature-dependent bands, starting with the negative band

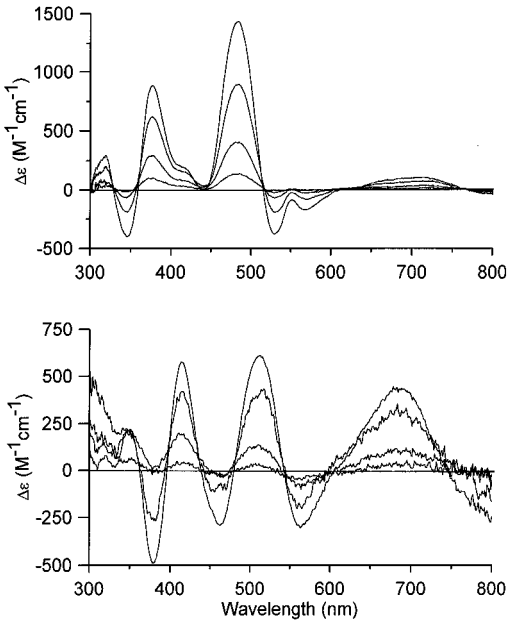

Figure 8. Comparison of the VTMCD spectra of the glycerol-induced and high-potential W(V) species in Pf AOR. Top panel: glycerol-inhibited W(V) species (W(V) spin concentration = 0.22 spins/W). The sample is described in Figure 2d and the spectra were recorded at temperatures of 1.68, 4.22, 9.8, and 18.6 K with a magnetic field of 4.5 T. Bottom panel: high-potential W(V) species (W(V) spin concentration = 0.30 spins/W). The sample was prepared adding 55% (v/v) glycerol to a sample poised at +309 mV (*vs* NHE) in a dye-mediated oxidative redox titration. The final sample concentration was 0.03 mM in AOR and the spectra were recorded at temperatures of 1.70, 4.22, 12.2, and 24.4 K with a magnetic field of 6.0 T. For both spectra, the intensity of all transitions increases with decreasing temperature.

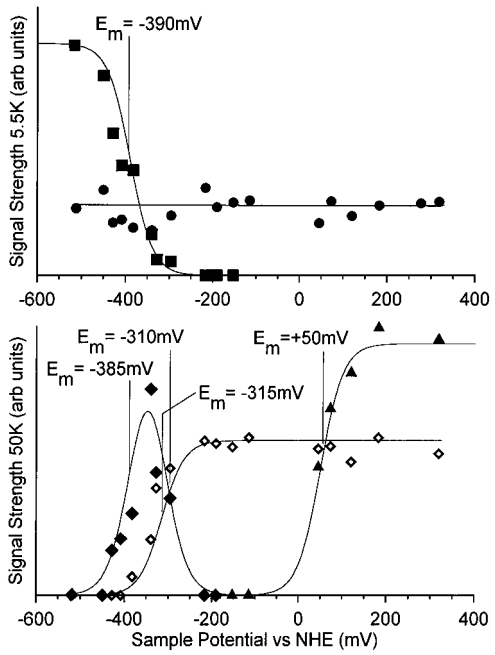

Figure 9. EPR signal intensities (arbitrary units) for ES-4 AOR as a function of poised potential. Dye-mediated redox titrations were carried out as described in the Experimental Section with active ES-4 AOR (0.04 mM) purified in the presence of 10% (v/v) glycerol. Upper panel: intensity of the $g = 4.7$ component of $S = {}^3/_2$ [4Fe−4S]$^+$ cluster (■) and the peak-to-trough intensity of the $g = 16$ resonance observed in the parallel-mode (●) at 5.5 K. Lower panel: peak-to-trough intensity of the $g = 1.900$ feature of the low potential W(V) species (◆), peak-to-trough intensity of the $g = 1.940$ component of the glycerol-inhibited W(V) species (◇), intensity of the $g = 1.890$ component of the high-potential W(V) species (▲), all measured at 50 K. Solid lines are best fits to one-electron Nernst equations or a two-electron Nernst equation for sequential one-electron oxidations with only the one-electron oxidized form EPR active. The midpoint potentials (*vs* NHE) used in constructing the Nernst plots are indicated on the figure. EPR conditions: temperatures as indicated; microwave power, 1 mW; modulation amplitude, 1.02 mT; microwave frequency, 9.60 GHz (perpendicular mode) and 9.37 GHz (parallel-mode).

centered at 880 nm, that are all assigned to S → W(V) charge transfer transitions on the basis of the MCD intensity. The appearance of intense low-energy S → W(V) charge transfer bands makes this spectrum distinct from that observed for either the spin-coupled or diol-inhibited W(V) species and suggests major changes in the nature of the coordinating S groups.

To establish if the magnetically isolated W(V) species discussed above are unique to Pf AOR, parallel oxidative EPR titrations were carried out for ES-4 AOR purified in the presence of 10% (v/v) glycerol. While the quality of the data is less than optimal due to the amount of sample available, resonances with g values and redox properties analogous to each of the three major magnetically isolated W(V) species in Pf AOR were identified, see Table 1. The redox behavior of the W(V) species monitored at 50 K and the $g = 16$ and the $S = {}^3/_2$ resonances monitored at 5.5 K are shown in Figure 9. The midpoint potential of the [4Fe−4S]$^{2+/+}$ couple, −390 ± 30 mV, is decreased by 50 mV compared to Pf AOR. Within experimental error, the intensity of the $g = 16$ resonance in parallel and perpendicular mode was invariant over the entire potential range, −440 to +300 mV, indicating a structural rather than a redox role for the metal center at the subunit interface. As for Pf AOR, a weak $g = 4.3$ resonance attributed to adventitiously bound Fe(III) ion appeared with a midpoint potential of +110 ± 30 mV. The low-field component of the low-potential W(V) species was obscured by radical species in the redox dyes, but the mid-field and high-field components are observed at $g =$ 1.900 and 1.860, respectively. The midpoint potentials for the appearance and disappearance of this resonance (E_m(W(IV)/W(V)) = −385 ± 30 mV and E_m(W(V)/W(VI)) = −310 ± 30 mV) are both increased by ∼50 mV compared to Pf AOR. The g values of the glycerol-induced W(V) species, $g = 1.961$, 1.940, 1.881, and the high-potential W(V) species, $g = 1.986$, 1.960, 1.890, are very similar to those in Pf AOR, but their potentials are shifted 40 mV more positive and 100 mV more negative, respectively. The 50-mV decrease in the [4Fe−4S]$^{2+/+}$ couple together with the 40-mV increase in the glycerol-induced W(IV)/W(V) couple relative to Pf AOR, explains why it was only possible to observe the VTMCD spectrum of the $S = {}^3/_2$ [4Fe−4S]$^+$ cluster without interference from the glycerol-induced W(V) species in dithionite-reduced samples of ES-4 AOR, but not in Pf AOR.

Discussion

The investigation of two closely related AORs from Pf and ES-4 with the combination of EPR and VTMCD spectroscopies has revealed major new insights into the properties of each type of metal site that has been identified and structurally characterized in X-ray crystallographic studies of Pf AOR.[6] The interpretation and implications of the spectroscopic results for each of the three sites are discussed separately below.

Mononuclear Metal Center. The most difficult metal site to investigate spectroscopically is the mononuclear metal site at the subunit interface. The X-ray crystal structure tentatively identified the metal as Fe on the basis of anomalous scattering and showed that it is coordinated in an approximately tetrahedral arrangement by two His and two Glu residues arranged in

H−X−X−E motifs in each subunit and is separated by ∼25 Å from either the [4Fe−4S] or W centers.[6] No parallel- or perpendicular-mode EPR signals attributable to a high-spin Fe(II) ($S = 2$) center were observed in samples of Pf AOR poised at potentials in the range −500 to +300 mV. However, monomeric high-spin Fe(II) sites ($S = 2$) are frequently rendered "EPR-silent" at X-band, as a result of zero-field splitting. In general, observation of an EPR resonance from a paramagnetic non-Kramers system is critically dependent on the spin state, the sign of the axial zero-field splitting parameter, D, and the rhombicity, E/D. A weak $g = 4.3$ resonance characteristic of a rhombic high-spin ($S = {}^5/_2$) Fe(III) center does appear with a midpoint potential of +110 mV in oxidative redox titrations of Pf AOR and ES-4 AOR. However, such resonances are invariably observed for Fe-containing proteins under oxidizing conditions and are usually attributed to adventitiously bound Fe(III). Such an assignment is also likely in AORs, since the appearance of the $g = 4.3$ resonance does not coincide with the loss of the "$g = 16$" resonance that is associated with the metal center at the subunit interface, see below. We conclude that the mononuclear metal site in Pf AOR is redox inactive over the potential range −450 to +300 mV.

In contrast to Pf AOR, a redox-invariant "$g = 16$" resonance from an integer spin paramagnet was observed in all samples of ES-4 AOR poised at potentials between −450 and +300 mV. This redox behavior rules out the possibility that this resonance arises from magnetic interaction between the $S = {}^3/_2$ [4Fe−4S]$^+$ cluster and a $S = {}^1/_2$ W(V) species. Hence it is attributed to the metal center at the subunit interface and the temperature-dependent behavior suggests assignment to a resonance within the lowest levels of the zero-field-split manifold. Although it occurs to lower fields than generally encountered for resonances within the $M_s = \pm 2$ "doublet" of $S = 2$, high-spin Fe(II) centers (crossovers typically in the range $g = 10-12$[19,21]), the resonant field for such resonances is critically dependent on the magnitude of the rhombic zero-field splitting.[19] A well-defined parallel-mode resonance with a crossover near $g = 16$ is certainly possible for a homogeneous $S = 2$ system ($D < 0$) with significant rhombic zero-field splitting. A rhombic splitting larger than the microwave energy (∼0.3 cm^{-1}) would preclude observation of the resonance at X-band, and such behavior and/or a change of sign of D, provides an explanation for the absence of this signal in Pf AOR. Relatively minor differences in the zero-field parameters could therefore account for the dramatically different EPR properties of the high-spin Fe(II) centers in these two enzymes and the absence of redox activity is consistent with a purely structural role.

There is, however, an alternative explanation for the origin of the "$g = 16$" resonance in ES-4 AOR. Very similar resonances with crossovers near $g = 16$ have been observed from the $S = 4$ ground states of ferromagnetically coupled diferrous centers in deoxyhemerythrin azide,[22] reduced methane monooxygenase,[23] reduced azide-bound ribonucleotide reductase,[24] and diferrous model complexes.[25] This raises the possibility that a carboxylate-bridged diferrous center may be at the subunit interface in ES-4 AOR. Observation of the characteristic $S = {}^1/_2$ EPR resonance associated with the mixed valence form,[26] would have provided strong evidence in support of this proposal, but it was not possible to effect oxidation at potentials up to +300 mV. It is intriguing to note that the H−X−X−E motif is a common feature of many diiron-containing proteins,[26] and close inspection of the structure of Pf AOR reveals a void where a second Fe site would be located if it was bridged by the two glutamates, with threoines side chains (Thr303) pointing toward the void. Replacement of Thr303 by His in ES-4 AOR might be all that is required to assemble a diiron site. Alternatively a head-to-tail rather than a head-to-head arrangement of the two subunits could conceivably accommodate a diiron site without any sequence modifications. The sequence and ultimately the X-ray crystal structure of ES-4 AOR will be required to assess the possibility of a structural diiron center in place of a mononuclear Fe site at the subunit interface of this enzyme.

[4Fe−4S]$^{2+,+}$ Cluster. The VTMCD and EPR studies reported here show that the [4Fe−4S]$^{2+,+}$ cluster in Pf and ES-4 AORs has unique electronic properties in the reduced state. While there are numerous examples of biological[15c,15d,27] and synthetic[28] [4Fe−4S]$^+$ clusters that have pure $S = {}^1/_2$ ground states or exists as a medium-dependent physical mixture of species with $S = {}^1/_2$ and ${}^3/_2$ ground states in frozen solutions, the clusters in AOR are the first examples with pure $S = {}^3/_2$ ground states. The ground state properties of the [4Fe−4S]$^+$ cluster in AORs are also invariant with pH (over the range pH 6−10) and are not affected by addition of up to at least 70% (v/v) glycerol or ethylene glycol. Moreover, due to the more axial zero-field splitting ($E/D = 0.12$, $D = 4$ cm^{-1}), the $S = {}^3/_2$ ground state for the [4Fe−4S]$^+$ clusters in AORs has ground properties quite distinct from those of any other $S = {}^3/_2$ [4Fe−4S]$^+$ cluster investigated thus far. As noted previously,[10] the ground state properties and resulting EPR spectrum are most similar to those of the dithionite-reduced $S = {}^3/_2$ nitrogenase FeMo cofactor cluster ($E/D = 0.05$, $D = +6$ cm^{-1})[29] or synthetic clusters with heteronuclear [Mo3Fe−4S] or [W3Fe−4S] cores ($E/D \sim 0.13$, $D \sim +1.5$ cm^{-1}).[30]

Room temperature magnetic susceptibility and/or NMR studies of nitrogenase Fe-protein[31] and Pf Fd[32] indicate the $S = {}^3/_2$ [4Fe−4S]$^+$ components are freezing artifacts. The

(21) (a) Hagen, W. R.; Dunham, W. R.; Johnson, M. K.; Fee, J. A. *Biochim. Biophys. Acta* **1985**, *828*, 369−374. (b) Werth, M. T.; Kurtz, D. M., Jr.; Howes, B. D.; Huynh, B. H. *Inorg. Chem.* **1989**, *28*, 1357−1361. (c) Werth, M. T.; Johnson, M. K. *Biochemistry* **1989**, *28*, 3982−3988.

(22) Hendrich, M. P.; Pearce, L. L.; Que, L., Jr.; Chasteen, N. D.; Day, E. P. *J. Am. Chem. Soc.* **1991**, *113*, 3039−3044.

(23) Hendrich, M. P.; Münck, E.; Fox, B. G.; Lipscomb, J. D. *J. Am. Chem. Soc.* **1990**, *112*, 5861−5865.

(24) Elgren, T. E.; Hendrich, M. P.; Que, L., Jr. *J. Am. Chem. Soc.* **1993**, *115*, 9291−9292.

(25) (a) Borovik, A. S.; Hendrich, M. P.; Holman, T. R.; Münck, E.; Papaefthymiou, V.; Que, L., Jr. *J. Am. Chem. Soc.* **1990**, *112*, 6031−6038. (b) Jang, H. G.; Hendrich, M. P.; Que, L., Jr. *Inorg. Chem.* **1993**, *32*, 911−919.

(26) (a) Nordlund, P.; Eklund, H. *Curr. Opin. Struct. Biol.* **1995**, *5*, 758−766. (b) Kurtz, D. M., Jr. In *Encyclopedia of Inorganic Chemistry*; King, R. B., Ed.; Wiley: U.K., 1994; Vol. 4, pp 1847−1859.

(27) (a) Lindahl, P. A.; Day, E. P.; Kent, T. A.; Orme-Johnson, W. H.; Münck, E. *J. Biol. Chem.* **1985**, *260*, 11160−11173. (b) Zambrano, I. C.; Kowal, A. T.; Mortenson, L. E.; Adams, M. W. W.; Johnson, M. K. *J. Biol. Chem.* **1989**, *264*, 20974−20983. (c) Onate, Y. A.; Vollmer, S. J.; Switzer, R. L.; Johnson, M. K. *J. Biol. Chem.* **1989**, *264*, 18386−18391. (d) Flint, D. H.; Emptage, M. H.; Finnegan, M. G.; Fu, W.; Johnson, M. K. *J. Biol. Chem.* **1993**, *268*, 14732−14742. (e) George, S. J.; Armstrong, F. A.; Hatchikian, E. C.; Thomson, A. J. *Biochem. J.* ***1989***, *264*, 275−284. (f) Flint, D. H.; Emptage, M. H.; Guest, J. R. *Biochemistry* **1992**, *31*, 10331−10337. (g) Kowal, A. T.; Werth, M. T.; Manodori, A.; Cecchini, Schröder, I.; Gunsalus, R. P.; Johnson, M. K. *Biochemistry* **1995**, *34*, 12284−12293.

(28) (a) Carney, M. J.; Papaefthymiou, G. C.; Spartalian, K.; Frankel, R. B.; Holm, R .H. *J. Am. Chem. Soc.* **1988**, *110*, 6084−6095. (b) Carney, M. J.; Papaefthymiou, G. C.; Whitener, M. A.; Spartalian, K.; Frankel, R. B.; Holm, R. H. *Inorg. Chem.* **1988**, *27*, 346−352. (c) Carney, M. J.; Papaefthymiou, G. C.; Frankel, R. B.; Holm, R. H. *Inorg. Chem.* **1989**, *28*, 1497−1503.

(29) Nelson, M. J.; Levy, M. A.; Orme-Johnson, W. H. *Proc. Natl. Acad. Sci. U.S.A.* **1983**, *80*, 147−150.

(30) (a) Holm, R. H.; Simhon, E. D. In *Molybdenum Enzymes*; Spiro, T. G., Ed.; John Wiley and Sons: New York, 1985; pp 1−87. (b) Carney, M. J.; Kovacs, J. A.; Zhang, Y.-P.; Papaefthymiou, G. C.; Spartalian, K.; Frankel, R. B.; Holm, R. H. *Inorg. Chem.* **1987**, *26*, 719−724.

(31) Meyer, J.; Gaillard, J.; Moulis, J.-M. *Biochemistry* **1988**, *27*, 6150−6156.

presence of a pure $S = {}^3/_2$ ground state, coupled with the lack of medium effects and the unique ground state parameters, argues in favor of the $S = {}^3/_2$ ground state being an intrinsic property of the $[4Fe-4S]^+$ cluster in AORs. However, further experiments are required to test this hypothesis. It is important to emphasize that a detailed understanding of the structural perturbations that dictate the ground state spin of a $[4Fe-4S]^+$ cluster has yet to emerge. There are examples of clusters with $S = {}^3/_2$ ground states that have complete cysteinyl coordination, e.g. AORs, nitrogenase Fe protein,[27a] *Bacillus subtilis* amidotransferase,[27c] and partial non-cysteinyl coordination, e.g. Pf Fd,[15c] *Desulfovibrio africanus* FdIII,[27e] *Escherichia coli* dihydroxyacid dehydratase,[27d] fumarase A,[27f] and mutant forms of fumarate reductase.[27g] The [4Fe−4S] cluster in Pf AOR is coordinated by four cysteines (Cys288, Cys291, Cys295, and Cys494) with three closely spaced in a $C-X_2-C-X_3-C$ arrangement.[6] However, the polypeptide conformation, even in the region of the closely spaced cysteines, is quite distinct from that found in crystallographically defined [4Fe−4S]-containing Fds.[6] The novel ground state properties are therefore likely to be a consequence of the unique protein conformation in the vicinity of the cluster and/or the H-bonding interactions that link the cluster to the pterin cofactor (Arg76 bridges these two groups by forming H-bonds to a cluster μ_3-S^{2-} and two sites on one of the pterin cofactors; the S_γ of Cys494 is H-bonded to one of the pterin ring nitrogens, N-8).[6]

Tungsten Center. Although EPR and VTMCD are limited to investigating paramagnetic W(V) species in Pf and ES-4 AORs, they have provided direct evidence for heterogeneity in the W center in active preparations and, as discussed below, they do facilitate assessment of the coordination environment in both active and inactive forms of the W center. Compared to the wealth of EPR data for Mo(V) centers in enzymes and oxo-thiolate model complexes, EPR studies of W(V) are limited to a handful of structurally characterized oxo-thiolate model complexes, see Table 2, and preliminary studies of some indigenous and substituted tungstoenzymes.[2,39−42] In order to utilize the extensive Mo(V) data, in addition to the available W(V) data, for interpretation of the EPR and VTMCD presented herein, the discussion of the structural origin of each of the W(V) species observed in this work is prefaced by a comparison of the electronic properties of Mo(V) and W(V) species in equivalent oxo-thiolate environments.

Mo(V) and W(V) have d^1 configurations and generally exhibit $S = {}^1/_2$ EPR resonances with $g_{av} < 2$ that are slow relaxing and observable at temperatures above 100 K. Larger deviations from the free-electron g value are expected and observed for W(V) compared to Mo(V) due to much larger spin−orbit coupling (spin−orbit coupling constants are typically 3−5 times larger for W than Mo).[33,43] This translates to greater g-value anisotropy and lower g_{av} values for W(V) compared to equivalent Mo(V) species. This is illustrated by the EPR data shown in Table 2 for synthetic oxo-thiolate-Mo(V) and -W(V) complexes and the pioneering study of W-substituted rat-liver sulfite oxidase (SO). Although W-substituted SO is inactive, the line shape, pH dependence, and anion dependence established for the Mo(V) species are mirrored by the W(V) species, indicating identical coordination environments.[2] In general these comparative EPR studies indicate that the overall line shape is preserved, albeit with amplified g-value anisotropy on substituting Mo by W. In addition, they show that the line widths are substantially larger (approximately doubled), the metal hyperfine is larger (^{183}W ($I = {}^1/_2$) *vs* ^{95,97}Mo ($I = {}^5/_2$)), and the resonances are less readily saturated for the equivalent W(V) species. The increased line width is particularly significant since it obscures proton hyperfine splitting. The close correspondence in the properties of W(V) and Mo(V) EPR resonances suggests that similar trends will also apply. Hence, an approximate correlation between the g_{av} value and the number of S-donor ligands is expected.[38]

Table 2. Comparison of EPR g Values and ^{183}W and ^{98}Mo A values ($cm^{-1} \times 10^4$) for Equivalent Oxothiolato-Mo(V) and W(V) Centers[a]

sample	g_{av}	A_{av}	g_1	g_2	g_3	A_1	A_2	A_3	ref
Models									
$[MoO(SPh)_4]^-$	1.990	32.3	2.017	1.979	1.979	52.3	22.3	22.3	33
$[WO(SPh)_4]^-$	1.936	55.1	2.018	1.903	1.903	78.1	44.4	44.4	33
$[MoO(SePh)_4]^-$	2.024	30.0	2.072	2.005	2.005	48.3	21.2	21.2	33
$[WO(SePh)_4]^-$	1.971	50.5	2.086	1.923	1.923	74.0	43.3	43.3	33
$[MoO(bdt)_2]^-$	1.994	28	2.023	1.986	1.977	45	n.d.	n.d.	34
$[WO(bdt)_2]^-$	1.960	50	2.044	1.931	1.911	74	40	37	34
$[MoO(edt)_2]^-$	2.004	29.6	2.052	1.983	1.979	49.4	18.7	20.7	38
$[WO(edt)_2]^-$	1.981	51.0	2.116	1.921	1.906	72.5	39.8	40.8	53
$[MoO(mnt)_2]^+$	1.986	27	2.015	1.982	1.960	41	5	36	36
$[WO(mnt)_2]^-$	1.959	n.d.	2.104	1.913	1.860	n.d.	n.d.	n.d.	37
Rat Liver Sulfite Oxidase									
low-pH Mo(V)	1.983	32.8	2.007	1.974	1.968	56.7	25.0	16.7	38
low-pH W(V)	1.91	∼54	1.98	1.89	1.87	81	∼41	∼41	2
high-pH Mo(V)	1.970	28.9	1.990	1.966	1.954	54.4	21.0	11.3	38
high-pH W(V)	1.88	n.d.	1.93	1.87	1.84	n.d.	n.d.	n.d.	2

[a] Abbreviations: n.d., not determined; bdt, 1,2-benzenedithioate; edt, 1.2-ethanedithiolate; mnt, (1,2-dicyanoethylene)dithiolate.

The larger spin−orbit coupling for W(V) is also expected to be manifest by significantly greater VTMCD intensity compared to the equivalent Mo(V) center, since MCD C-term intensity is directly dependent on excited-state spin−orbit coupling. At present VTMCD studies of relevant Mo(V) species are limited to the diol-inhibited desulfo form of xanthine oxidase (XO) (mono-dithiolene coordination),[16c] diol-inhibited Rs DR[16a] and the corresponding proton-split Mo(V) species in Rs DR[16b] (both bis-dithiolene coordination), and model complexes with mono-dithiolate coordination,[44] i.e. [LMoO(SCH_2CH_2S)] and [LMoO-(toluene-3,4-dithiolate)] (L = hydrotris(3,5-dimethyl-1-pyrazolyl)-borate). In all cases the visible VTMCD bands have been assigned exclusively or in large part to S → Mo(V) charge transfer transitions. Although the X-ray crystal structure of Pf AOR indicates that the mono-dithiolate and mono-dithiolene species are unlikely to be appropriate models for the W-AOR active site,[6] these Mo(V) VTMCD studies do indicate that the VTMCD intensity is critically dependent on the number of S-donor ligands. Under comparable conditions, the VTMCD intensity normalized to the Mo(V) spin concentration increases at least 10-fold on going from two to four S-donor ligands and a similar trend is expected for W(V) centers.

(32) Calzolai, L.; Gorst, C. M.; Zhao, Z.-H.; Teng, Q.; Adams, M. W. W.; LaMar, G. N. *Biochemistry* **1995**, *34*, 11373−11384.
(33) Hanson, G. R.; Brunette, A. A.; McDonell, A. C.; Murray, K. S.; Wedd, A. G. *J. Am. Chem. Soc.* **1981**, *103*, 1953−1959.
(34) Oku, H.; Ueyama, N.; Nakamura, A. *Chem. Lett.* **1995**, 621−622.
(35) Ellis, S. R.; Collison, D.; Garner, C. D.; Clegg, W. *J. Chem. Soc., Chem. Commun.* **1986**, 1483−1485.
(36) Das, S. K.; Chaudhury, P. K.; Biswas, D.; Sarkar, S. *J. Am. Chem. Soc.* **1994**, *116*, 9061−9070.
(37) W(V) species formed *in situ* by oxidation of W(IV) complex with I_2. Oku, H.; Ueyama, N.; Nakamura, A.; Johnson, M. K. Unpublished results.
(38) Dhawan, I. K.; Enemark, J. H. *Inorg. Chem.* **1996**, *35*, 4873−4882.
(39) Deaton, J. C.; Solomon, E. I.; Watt, G. D.; Wetherbee, P. J.; Durfor, C. N. *Biochem. Biophys. Res. Commun.* **1987**, *149*, 424−430.
(40) Schmitz, R. A.; Albracht, S. P. J.; Thauer, R. K. *FEBS Lett.* **1992**, *309*, 78−81.
(41) Huber, C.; Caldeira, J.; Jongejan, J. A.; Simon, H. *Arch. Microbiol.* **1994**, *162*, 303−309.
(42) Hensgens, C. M. H.; Hagen, W. R.; Hansen, T. A. *J. Bacteriol.* **1995**, *177*, 6195−6200.
(43) Kon, H.; Sharpless, N. E. *J. Phys. Chem.* **1966**, *70*, 105−111.
(44) Carducci, M. D.; Brown, C.; Solomon, E. I.; Enemark, J. H. *J. Am. Chem. Soc.* **1994**, *116*, 11856−11868.

Spin-Coupled W(V). Previous EPR studies indicated that the broad complex resonance seen in dithionite-reduced inactive Pf RTP resulted from weak spin−spin interaction between a $S = {}^3/_2$ species and a lower potential center that becomes paramagnetic only on one-electron reduction and is present in an approximate 1:1 stoichiometry.[10] The present work shows that the $S = {}^3/_2$ center is the $[4Fe-4S]^+$ cluster and that the lower potential species is a $S = {}^1/_2$ W(V) species. In RTP, all the W has been converted into the W(VI)/W(V) species that gives rise to the spin-coupled W(V) resonance and this accounts for the absence of a magnetically isolated W(V) species during oxidative titrations. An analogous spin-coupled W(V) resonance is observed in active samples of Pf AOR and in some samples of ES-4 AOR, but it corresponds to <20% of the W in the enzyme. Inactivation of active samples of Pf and ES-4 AOR by prolonged exposure to air, followed by re-reduction with dithionite did not change the amount of this species. Therefore, although this form of W is clearly catalytically inactive, it should not be equated with the product of O_2 inactivation. Rather it seems to be the product of some form of reductive inactivation that results from prolonged exposure to dithionite during the purification procedure.

Our current working hypothesis for the nature of this inactive species is that it involves reductive loss of one of the two pterin dithiolene ligands. The recent X-ray crystal structure of Rs DR[9] has shown one of the two pterin dithiolene Mo ligands is reductively labile, and it has been proposed that one set of Mo(V) EPR signals (low-g type 1 and type 2)[45] results from a species that has lost one of the two pterin dithiolene ligands and gained an oxo group.[46] Our reasoning is as follows. First, the W-XAS data indicates an extra oxo ligand and a decrease by one or two in the number of S-donor ligands at approx 2.4 Å for Pf RTP compared to active AOR.[11,13] The coordination sphere of W in Pf RTP comprises two W=O at 1.74 Å, approximately three W−S ligands at 2.41 Å and possibly an additional W−O or W−N ligand at 2.1 Å.[11] Second, the intensity of the VTMCD spectrum corresponding to the spin-coupled W(V) species is at least an order of magnitude less (on a per W(V) basis) than those of either the diol-inhibited or the high-potential W(V) species. As discussed above, this is indicative of loss of a pterin dithiolene ligand. Third, the available redox data indicate reduction of the spin-coupled W(V) species to the W(IV) state does not occur at potentials down to −600 mV.[10] The available model complexes indicate that bis-dithiolene coordination is likely to be a requirement for stabilizing the W(IV) state at physiologically relevant potentials.[47] Hence the loss of a pterin dithiolene ligand might be expected to result in loss of catalytic activity due to the inability of achieving reduction to the W(IV) state.

These considerations and the recent X-ray crystallographic data for dithionite-reduced Rs DR[9] form the basis for the proposed structure for the inactive spin-coupled W(V) species shown in Figure 10. Partial loss of one of the dithiolene ligands is proposed to proceed by keto−enol tautomerization following protonation of the thiolate. The structure is shown as a monooxo-W(V) species (originating from a dioxo-W(VI) form), although the possibility of a novel dioxo-W(V) species cannot be excluded since at least 50% of the W in the Pf RTP samples used for W-XAS was in the spin-coupled W(V) state. Dioxo-Mo(V) centers exhibit very characteristic EPR properties with

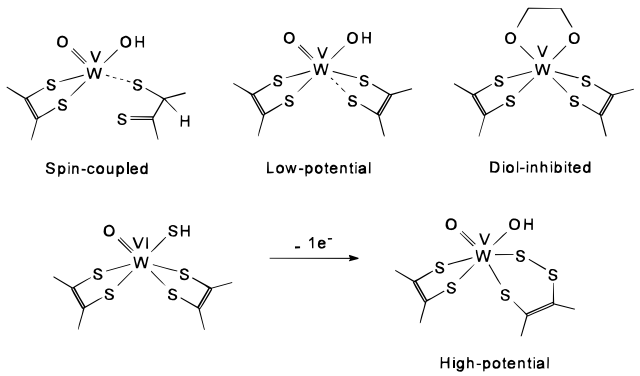

Figure 10. Proposed structures for the spin-coupled, low-potential, diol-inhibited and high-potential W(V) species in W-AORs. The high-potential W(V) species is proposed to originate from a W(VI) species via a net one-electron oxidation involving a two-electron ligand-based oxidation and a one-electron metal-based reduction.

highly anisotropic spectra and low g_{av} values (e.g., from the crystallographically defined complex $[LMoO_2(SPh)]^-$ (L = hydrotris(3,5-dimethyl-1-pyrazolyl)borate), $g = 1.991, 1.931, 1.843$).[48] Unfortunately spin−spin interaction with a higher potential $[4Fe-4S]^+$ cluster prevents direct assessment of the g-value anisotropy for the spin-coupled W(V) species in Pf AOR. However, it is interesting to note that novel highly anisotropic W(V) resonances with similar properties (i.e., from inactive W(VI)/W(V) species and involved in spin−spin interaction with a $[4Fe-4S]^+$ cluster) are observed in two other members of the W-AOR family of enzymes. Recent spectroscopic studies Pf GAPOR revealed a W(V) resonance with $g = 1.954, 1.890, 1.830$, in anaerobically isolated samples that were reduced and inactivated by dithionite.[49] This W(V) species undergoes spin−spin interaction with a lower potential $S = {}^1/_2$ $[4Fe-4S]^+$ cluster. Two very similar W(V) resonances, $g = 1.943, 1.902, 1.850$ and $g = 1.949, 1.889, 1.844$, have been reported in dithionite-reduced samples of Dg AOR.[42] These resonances disappear at lower potentials and are replaced by a broad fast-relaxing resonance, attributed to a $S = {}^1/_2$ $[4Fe-4S]^+$ interacting with a nearby paramagnetic species. The authors rationalized this behavior in terms of magnetic interaction involving a $S = 1$ W(IV) species.[42] However, paramagnetic W(IV) is *extremely* unlikely in a low symmetry biological environment and loss of the magnetically isolated W(V) resonances at lower potentials due to spin−spin interaction with a lower potential $[4Fe-4S]^+$ cluster is a far more plausible explanation in light of the studies presented herein. The low g_{av} values for these resonances, 1.89−1.90, indicate fewer sulfur donor ligands than any magnetically isolated W(V) species in Pf or ES-4 AOR, and it seems likely that these resonances correspond to the spin-coupled W(V) species in Pf AOR. Assignment to a monooxo-W(V) species is therefore more reasonable, since the g-value anisotropy is not particularly high compared to other W(V) resonances and the lower g_{av} value is readily rationalized in terms of fewer S-donor ligands.

Low-Potential W(V). All the available evidence indicates that the low-potential W(V) species in Pf and ES-4 AOR, $g \sim 1.99, 1.90, 1.86$, see Table 1 and Figure 6a, corresponds to a catalytically active form of W that accounts for 20−30% of the total W content. First, this form of W can cycle between W(IV)/W(V)/W(VI) oxidation states at potentials that are physiologically relevant with W(V) species maximal at −400

(45) Bennett, B.; Benson, N.; McEwan, A. G.; Bray, R. C. *Biochem. J.* **1994**, *255*, 321−331.
(46) George, G. N.; Hilton, J.; Rajagopalan, K. V. *J. Am. Chem. Soc.* **1996**, *118*, 1113−1117.
(47) (a) Ueyama, N.; Oku, H.; Nakamura, A. *J. Am. Chem. Soc.* **1992**, *114*, 7310−7311. (b) Das, S. K.; Biswas, D.; Maiti, R.; Sarkar, S. *J. Am. Chem. Soc.* **1996**, *118*, 1387−1397.
(48) Xiao, Z.; Gable, R. W.; Wedd, A. G.; Young, C. G. *J. Am. Chem. Soc.* **1996**, *118*, 2912−2921 and references therein.
(49) Mukund, S.; Koehler, B. P.; Roy, R.; Adams, M. W. W.; Johnson, M. K. Unpublished observations.

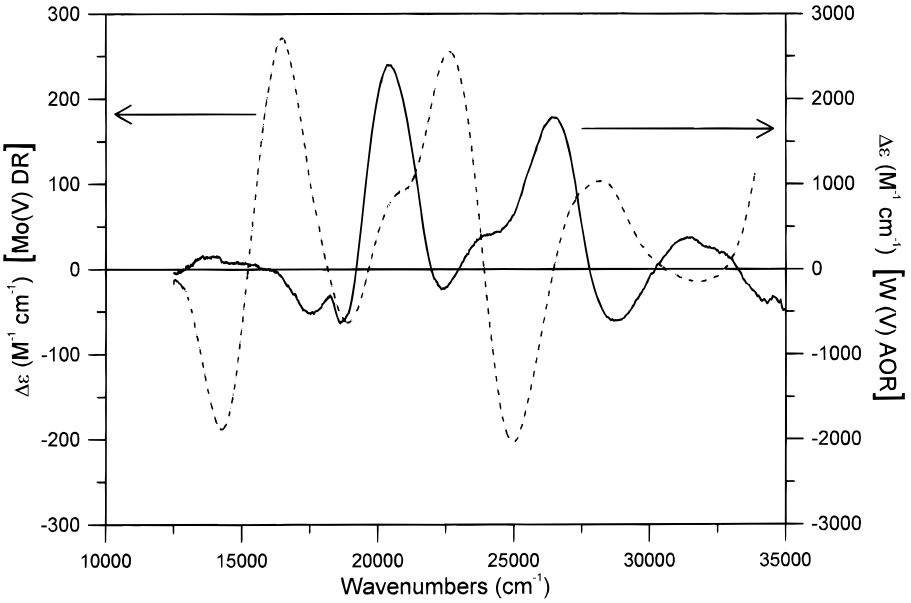

Figure 11. Comparison of the VTMCD spectra of the W(V) center in ethylene glycol-treated Pf AOR with the Mo(V) center in glycerol-inhibited *R. sphaeroides* DMSO reductase. Solid line: glycol-induced W(V) center in AOR. Sample is as described in Figure 2e. Dashed line: Mo(V) center in DMSO reductase. Data taken from ref 15a. Spectra collected at 4.2 K with a magnetic field of 4.5 T. $\Delta\epsilon$ values are based on W(V) or Mo(V) concentrations as determined by EPR spin quantitations.

mV in Pf AOR and −350 in ES-4 AOR. Second, this resonance is observed in samples treated anaerobically with substrate under physiological conditions, 85 °C, and then frozen rapidly for EPR. Third, it is the only resonance that is lost, together with enzymatic activity, when AORs are treated anaerobically at 85 °C with high concentrations (55% (v/v)) of diols such as glycerol or ethylene glycol. Fourth, while redox cycling of this species is reversible for potentials in the range −500 to 0 mV, this W(V) resonance is not observed and enzymatic activity is irreversibly lost in samples that have been exposed to O_2 or anaerobically oxidized to +300 mV. In its place, re-reduced samples of Pf AOR have been found to exhibit two new W(V) resonances that are maximal at approximately −190 mV, $g = 2.021, 1.988, 1.957$ (re-reduced 1) and $g = 1.949, 1.916, 1.850$ (re-reduced 2).

Our current working model for the structure of the low-potential W(V) species is shown in Figure 10. It involves W coordination by three dithiolene sulfurs with the fourth only weakly attached, in addition to a single oxo and hydroxyl ligand. In large part this model is based on the similarity in the g-values with those of the low pH W(V) species in W-substituted SO,[2] see Tables 1 and 2, and the available crystallographic data for Pf AOR.[6] Recent mutagenesis results,[50] coupled with the EPR and Mo-XAS data,[51] have provided strong evidence for a Mo-(V) coordination sphere in SO involving one oxo, one hydroxyl, one chloride (present only in the low-pH form), one cysteinyl sulfur, and two sulfurs from the a pterin dithiolene. The suggestion that one of the dithiolene sulfurs is only weakly coordinated originates from the recent crystal structure of Rs DR[9] and is tentatively supported by the correspondence with W-substituted SO and the g_{av} value which is significantly lower than for crystallographically defined oxo-W(V) model complexes with bis-dithiolene or four thiolate ligands, see Tables 1 and 2. Further work involving the effect pH, D_2O/H_2O exchange, and the presence of anions such as fluoride, chloride, or phosphate, will be required to test the model and such studies are in progress.

Diol-Inhibited W(V). The active W species responsible for the low-potential W(V) resonance in Pf and ES-4 AOR is irreversibly and quantitatively converted into a diol-inhibited form by the addition of high concentrations of glycerol or ethylene glycol at physiological temperatures. The conversion occurs at least partially at room temperature and this precludes VTMCD studies of low-potential W(V) species, since the glycerol or ethylene glycol are required to form a low-temperature glass and the diol-inhibited forms have very intense VTMCD spectra. This diol-inhibited form exhibits a characteristic W(V) resonance (E_m(W(IV)/W(V)) = −350 mV in Pf AOR and −315 mV in ES-4 AOR) that is dependent on the specific diol, i.e. $g = 1.965, 1.941, 1.884$ for the glycerol-induced W(V) species and $g = 1.958, 1.938, 1.887$ for the glycol-induced W(V) species in Pf AOR, and persists at potentials up to at least +100 mV, see Table 1 and Figures 5 and 6b. Partial (10−20%) conversion to the glycerol-inhibited form also occurs in AORs purified in the standard purification and storage buffer which contains 10% (v/v) glycerol. These results facilitate interpretation of the remaining two W(V) resonances observed in dithionite-reduced Dg AOR, $g = 1.974, 1.932, 1.869$ and $g = 1.962, 1.921, 1.874$.[42] The sample was purified in the presence of 9% (v/v) glycerol and the g values identify both resonances as originating from glycerol-induced W(V) species. Analogous glycerol-inhibited W(V) species provide direct evidence that these enzymes have a common W active site structure.

A very similar glycerol-inhibited Mo(V) species, i.e. g-value anisotropy consistent with Mo/W substitution without change in coordination type or geometry, has been observed in Rs DR, $g = 1.990, 1.984, 1.962$.[16a,46] Moreover, the similarity extends to the excited state electronic structure as revealed by VTMCD studies, see Figure 11. Both the glycerol-inhibited Mo(V) center in Rs DR and the glycerol- or glycol-inhibited W(V) species in Pf AOR exhibit an analogous pattern of temperature-dependent MCD bands with corresponding transitions shifted up in energy by ∼4000 cm^{-1} for W relative to Mo. Prior to the discovery that the Mo center in Rs DR was coordinated by the dithiolenes

(50) Garrett, R. M.; Rajagopalan, K. V. *J. Biol. Chem.* **1996**, *271*, 7387−7391.

(51) (a) George, G. N.; Kipke, C. A.; Prince, R. C.; Sunde, R. A.; Enemark, J. H.; Cramer, S. P. *Biochemistry* **1989**, *28*, 5075−5080. (b) George, G. N.; Garrett, R. M.; Prince, R. C.; Rajagopalan, K. V. *J. Am. Chem. Soc.* **1996**, *36*, 8586−8592.

of two pterin cofactors with guanine dinucleotides,[9,52] we had tentatively assigned the visible VTMCD spectrum of the glycerol-inhibited Mo(V) center in Rs DR exclusively to π-dithiolene-to-Mo(V) charge transfer transitions from a single coordinated dithiolene.[16a] This assignment requires revision to account for two dithiolene ligands and detailed assignments with parallel studies of structurally characterized dithiolene- and dithiolate-coordinated Mo(V) and W(V) complexes will be presented elsewhere.[53] It is sufficient here to note that the alternating pattern of $-+-+-+$ MCD bands with increasing energy, can be rationalized exclusively in terms of S(π)-to-Mo-(V) charge transfer transitions from two equivalent dithiolene ligands under C_{2v} symmetry. The diol-inhibited W(V) VTMCD spectrum can be assigned in the same way with the higher energies due to the increase in energy of the W 5d orbitals. As expected on the basis of larger spin−orbit coupling, the intensities of the corresponding transitions (normalized to the Mo(V) and W(V) concentrations as assessed by EPR spin quantitations) are an order of magnitude larger for W.

The close similarity in the ground and excited state electronic properties of the diol-inhibited Mo(V)/W(V) forms of Rs DR and Pf AOR dictates very similar coordination environments. Hence the proposed structure for the diol-inhibited W(V) species in AORs shown in Figure 10, is based largely on the recent Mo-XAS data for the glycerol-inhibited Mo(V) form of Rs DR,[46] and the X-ray structures of Rs DR[9] and Pf AOR.[6] The intense VTMCD and the increase in g_{av} values relative to the low-potential W(V) and spin-coupled W(V) species are consistent with bis-dithiolene coordination. In addition the observation that the EPR and VTMCD spectra are sensitive to the specific diol adds further support for direct diol coordination of the W center.

High-Potential W(V). EPR redox titrations of Pf AOR revealed two additional W(V) species that appeared at higher potentials. The mid-potential W(V) species, $g = 1.988, 1.961, 1.940$, accounting for <0.03 spins/W, appeared with a midpoint potential of −345 mV and persisted up to at least +100 mV. The origin of this minor species is unclear at present and will not be discussed further. At still higher potentials, the high-potential W(V) species, $g \sim 1.98-1.99, 1.96, 1.89$, accounting for ~0.3 spins/W, appeared with a midpoint potential of +157 mV in Pf AOR and +50 mV in ES-4 AOR, and persisted up to at least +300 mV. Moreover, an analogous resonance is also present in the W-containing CAR from *Clostridium thermoaceticum* (Ct), as purified anaerobically but in the absence of dithionite, $g = (2.035), 1.959, 1.899$.[41] The low-field g value has been incorrectly assigned in this case due to overlap with unidentified resonances in the $g = 2$ region. This result is important since it attests to an analogous W active-site structure in this enzyme.

In both AORs, the high-potential W(V) species is a major component corresponding to approximately 30% of the W in the enzyme. However, it is not a catalytically viable W(V) species and the available evidence indicates that it originates from a W species quite distinct from that responsible for the low-potential W(V) species. The main evidence for this is that it is also observed without change in intensity or redox properties in samples that have been irreversibly inactivated by prolonged exposure to O_2 or a large excesses of glycerol. Moreover, such a high-potential redox process cannot be physiologically relevant in light of the extremely low potentials of acid/aldehyde couples, <−500 mV, and is unlikely to involve a W(IV)/W(V) couple. We have therefore considered the possibility of ligand based redox chemistry. Dithiolenes are redox active ligands and can undergo two-electron oxidation to give the neutral form with two C=S bonds:

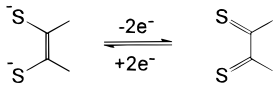

Such a two-electron ligand oxidation coupled with one-electron reduction of a W(VI) species would result in a W(V) species effectively coordinated by only one pterin dithiolene. However, the high g_{av} value and the intense VTMCD spectrum argue strongly in favor of coordination by four S-donor ligands. The VTMCD spectrum comprises four alternating positive and negative bands extending to much lower energy than the diol-inhibited W(V) species. Our current interpretation is that these correspond to the eight possible S(π)-to-W(V) charge transfer transitions to the lowest energy d orbital with the greater spread in energy, compared to the diol-inhibited W(V) species, resulting from much greater heterogeneity in the nature of the S-donor ligands.

One possibility that is consistent with the observed properties of the high-potential species is shown in Figure 10. This requires a terminal S ligand (S^{2-} or SH^-) which undergoes two electron oxidation and insertion into one of the W−S(dithiolene) bonds concomitant with a one-electron reduction of a W(VI) species to give a net one-electron oxidation. The resulting species has heterogeneity in the S-donor ligand set and would be expected to have low-energy S → W(V) charge transfer from the coordinated disulfide. Such ligand based redox chemistry is not without precedence in the chemistry of thio-Mo centers.[54] W-XAS or X-ray crystallography has not shown any evidence for a terminal sulfido ligand, although this might be difficult to detect if it was present on only 30% of the W. However, W-XAS studies of active dithionite-reduced Pf AOR do indicate four or five W−S ligands at 2.41 Å.[13]

Summary and Conclusions. The overall picture that has emerged from the EPR and VTMCD studies of Pf and ES-4 AOR is that the W center is not homogeneous in the samples as prepared. In both there are at least two major components, each corresponding to approximately 30% of the W in the enzyme and each coordinated by two pterin dithiolenes. One of these cycles between the W(IV)/W(V)/W(VI) states at physiologically relevant potentials and is responsible for the low-potential W(V) resonance. It appears to be associated with active enzyme, since the low-potential W(V) species is not observed in samples subjected to reductive or oxidative inactivation. The other is most likely a W(VI) species with a terminal S ligand that gives rise to the high-potential W(V) species at nonphysiologically relevant potentials (>0 mV) via a ligand based oxidation. It is unclear at present if this W(VI) species is catalytically competent under physiological conditions. In addition, purified samples of active AORs can have up to 20% of the W as a reductively inactivated species that is probably ligated by only one pterin dithiolene, is responsible for the spin-coupled W(V) species, and cycles between the W(VI)/W(V) states with a midpoint potential close to −450 mV. The available X-ray crystallographic and W-XAS data for dithionite reduced Pf AOR are therefore likely to correspond to average structures with W(IV), W(V) and W(VI) species all contributing. There is clearly a pressing need to formulate

(52) Hilton, J. C.; Rajagopalan, K. V. *Arch. Biochem.* **1996**, *325*, 139−143.

(53) Oku, H., Koehler, B. P.; Ueyama, N.; Nakamura, A.; Johnson, M. K. Manuscript in preparation.

(54) (a) Pan, W.-H.; Harmer, M. A.; Halbert, T. R.; Stiefel, E. I. *J. Am. Chem. Soc.* **1984**, *106*, 459−460. (b) Draganjac, M.; Simhon, E.; Chan, L. T.; Kanatzidis, M.; Baenziger, N. C.; Coucouvanis, D. *Inorg. Chem.* **1982**, *21*, 3321−3326.

preparations of homogeneous active enzymes as well as to investigate the effects of high concentrations of anions such as sulfide that are present under physiological growth conditions. For example, by analogy with xanthine oxidase, it is possible that the low-potential W(V) species corresponds to a slow or desulfo form of the enzyme with the rapid form corresponding to a mixed oxo-thio-W(VI) species. Such experiments and additional spectroscopic studies to test the structures proposed in Figure 10 are currently in progress.

Classes of Tungstoenzymes. On the basis of similarities in at least one W(V) EPR resonance, a common active site structure is proposed for Pf and ES-4 AORs, Pf GAPOR, Ct CAR, and Dg AOR. The high sequence homology between Pf AOR and FOR from *Thermococcus litoralis* (Tl),[55] coupled with chemical analysis data for Pf and Tl FOR (i.e., one W and four Fe, non-nucleotide form of the pterin cofactor),[56] suggests an analogous active site structure in FORs. (Detailed spectroscopic studies of Tl FOR are currently in progress.) Hence the available evidence suggests a large class of W-AORs, typified by structurally characterized Pf AOR,[6] each with a $[4Fe-4S]^{2+,+}$ cluster and a nearby W center coordinated by the dithiolenes of two non-nucleotide pterin cofactors, but with no protein ligands. On the basis of the limited EPR and sequence data that is available for W-FDH[57] and W-FMDH[58] enzymes, it has been proposed[5c] that they correspond to a different class of W-enzyme with an active site comprising W coordinated by the dithiolenes of two pterin cofactors with guanine dinucleotide side chains, and one protein ligand (Se-Cys for Ct FDH and Cys for the W-FMDHs from methanogenic archaea). The Mo-containing Rs DR is the structural prototype for this class of W enzyme,[9] with Ser as the protein ligand to the metal in this case. The anomalous W(V) EPR signals exhibited by these enzymes, i.e. high g_{av} values and at least one g value of >2.0023, ($g =$ 2.101, 1.980, 1.950 in Ct FDH poised at -450 mV[57c] and $g =$ 2.049, 2.012, 1.964 in air-oxidized inactive samples of the substituted FMDH from *Methanobacterium wolfei*[58a]) are certainly consistent with an additional S or Se ligand from Se-Cys or Cys.

Acknowledgment. This work was supported by Grants from the National Science Foundation (MCB9419019 to M.K.J.), the Department of Energy (FG09-88ER13901 to M.W.W.A.), and a National Science Foundation Research Training Group Award to the Center for Metalloenzyme Studies (BIR-9413236). We thank Professor D. M. Kurtz, Jr., for helpful discussions concerning diiron proteins and Prof. R. L. Belford for the EPR simulation program QPOW.

Supporting Information Available: MCD saturation magnetization plots for dithionite-reduced ES-4 AOR, Pf RTP, and Pf AOR treated with formaldehyde and glycerol at 80 °C and EPR spectra recorded at selected potentials during oxidative and reductive dye-mediated redox titrations of Pf AOR (7 pages). See any current masthead page for ordering and Internet access instructions.

JA962197U

(55) Kletzin, A.; Mukund, S.; Kelley-Crouse, T. L.; Chan, M. K.; Rees, D. C.; Adams, M. W. W. *J. Bacteriol.* **1995**, *117*, 4817−4829.

(56) (a) Mukund, S.; Adams, M. W. W. *J. Biol. Chem.* **1993**, *268*, 13592−13600. (b) Johnson, J. L.; Rajagopalan, K. V.; Mukund, S.; Adams, M. W. W. *J. Biol. Chem.* **1993**, *268*, 4848−4852.

(57) (a) Cramer, S. P.; Liu, C.-L.; Mortenson, L. E.; Spence, J. T.; Liu, S.-M.; Yamamoto, I.; Ljungdahl, L. G. *J. Inorg. Biochem.* **1985**, *23*, 119−124. (b) Yamamoto, I.; Saiki, T., Liu, S.-M.; Ljungdahl, L. G. *J. Biol. Chem.* **1983**, *258*, 1826−1832. (c) Deaton, J. C.; Solomon, E. I.; Watt, G. D.; Wetherbee, P. J.; Durfor, C. N. *Biochem. Biophys. Res. Commun.* **1987**, *149*, 424−430.

(58) (a) Schmitz, R. A.; Albracht, S. P. J.; Thauer, R. K. *FEBS Lett.* **1992**, *309*, 78−81. (b) Hochheimer, A.; Schmitz, R. A.; Thauer, R. K.; Hedderich, R. *Eur. J. Biochem.* **1995**, *234*, 910−920.